Working at Higher Magnifications in Scanning Electron Microscopy with Secondary and Backscattered Electrons on Metal Coated Biological Specimens and Imaging Macromolecular Cell Membrane Structures

Klaus-Ruediger Peters
Yale University

Recommended Citation

Utah State University
MERRILL-CAZIER LIBRARY

WORKING AT HIGHER MAGNIFICATIONS IN SCANNING ELECTRON MICROSCOPY
WITH SECONDARY AND BACKSCATTERED ELECTRONS ON METAL COATED BIOLOGICAL SPECIMENS AND
IMAGING MACROMOLECULAR CELL MEMBRANE STRUCTURES

Klaus-Ruediger Peters

Department of Cell Biology
Yale University School of Medicine
333 Cedar Street, New Haven, CT 06510-8002
Phone No.: (203) 785-4306

Abstract

Membrane structures of macromolecular dimensions were imaged with high resolution secondary electron type I (SE-I) signal contrasts on metal coated biological specimens. The quality of the surface information was strongly dependent on the signal used for microscopy and on the properties of metal films, i.e., thickness, continuity, structure and decoration effects. Films of 10 nm thickness produced so much type II electrons that identical images were obtained with the conventional SE-II and BSE-II signals. In such images, the type I SE signal was so low that only very weak contrasts were recognizable. If the films - continuous or discontinuous - were composed of large metal aggregates (gold and platinum) a strong micro-roughness contrast was produced by the type II signal. At high magnifications (100,000 x) this background signal greatly reduced the S/N ratio of the SE-I signal. A similar effect was previously shown to be produced by the type III background signal. The type II background signal minimized when continuous films of small aggregates (tantalum and chromium) were applied. SE-I contrast dominated in the image if the film thickness was limited to 1 nm. Additionally, it was found that gold and platinum decorated membrane surface structures, <20 nm in size, and did not reveal all the topographic information available (size, shape, orientation spacing of small surface features) but merely displayed center-to-center distances. These decoration effects were avoided and extensive topographic information was obtained through surface coating with Ta or Cr.

Introduction

In recent years, high magnification scanning electron microscopy (SEM) has challenged transmission electron microscopy (TEM) as a means of obtaining high resolution images of the surface of biological specimens. Conventional TEM is bound to platinum-carbon replication of the specimens since only platinum resists the cleaning procedures used in the replica technique to remove all of the specimen beneath the replica. The topographic resolution of such replicas is not limited by the instrumental resolution but by the inability of platinum (deposited at temperature >100 K) to "replicate" or coat small macromolecular fine structure on surfaces. In SEM, metals other than platinum can be used to pattern even the smallest surface details since the metal film is visualized directly on the specimen's surface without further treatment. The resolution is only limited by instrumental parameters and is improved sufficiently in modern scanning electron microscopes if they are equipped with high brightness electron guns and are operated in a high resolution imaging mode.

The imaging theory for SEM covers the generation and collection of the signal as well as the generation of contrasts. Both aspects were already studied for conventional SEM (Kanter, 1957; Everhart et al., 1959; Seiler, 1967; Reimer et al., 1968; Drescher et al., 1970) as well as for high magnification SEM (Broers, 1969 and 1970; Wells, 1971; Koike et al., 1971; Wells, 1974; Watabe et al., 1976; Peters, 1982a and b; Seiler, 1983; Peters, 1984a and b) using secondary electrons (SE) or backscattered electrons (BSE).

However, only recently the generation of SE contrasts in images of high magnification was investigated in detail. High magnification topographic contrasts provided a good qualitative and quantitative assay for high resolution type I signals (George and Robinson, 1977a). Conventional imaging (George and Robinson, 1976 and 1977b; Pawley, 1984) failed to produce high resolution signal contrasts and conventional Monte Carlo computation seemed to overestimate the signal's strength (Seiler, 1983). Development of a special signal collection procedure to enrich the high resolution SE signal (Peters, 1982a and 1984a) and revised calculations of expected signal strength (Joy, 1984) made it possible to establish a new

imaging theory for the high resolution SE signal (Peters, 1984b) and to reevaluate conventional imaging procedures.

For a visualization of small surface details at high magnifications, a probe size smaller than the dimensions of the feature size and a high electon density in the probe's cross section (brightness) are necessary to generate an adequate signal. Additionally, the background component of the signal has to be reduced because of its noise contribution (Everhart et al., 1959; Peters, 1984a). The amplitude of background signal variations is often larger than the contrasts of fine structures and thus small details of low contrasts are obscured and not imaged (Peters, 1982a). Two strategies to reduce the background contribution are used. First, the surface details are imaged at a glancing angle of the probe on the surface of a highly tilted specimen so as to image against an empty background. This was realized with SE signals (Broers, 1969 and 1970). Then, the same approach was extended to BSE imaging using a low take-off angle (angle between detector axis and specimen surface; Wells et al., 1974; Wells, 1979). Secondly, the background is filtered out (Wells, 1971). Energy filtering was adequate for BSE (Wells et al., 1973; Broers et al., 1975) but not applicable for SE. However, the background can be reduced and contrast structures of the remainder smoothened to such an extent that high resolution SE contrasts are imaged in analytical microscopes (Koike et al., 1971 and 1973) as well as in standard microscopes (Peters, 1982a, b and 1984a).

To overcome the limitations set for resolution on bulk samples by the range of the electrons collected in the signal, metal coating must be applied with a thickness thinner than the range of the critical signal electrons (Everhart and Chung, 1972). This proposal is realized in this paper on bulk biological specimens for the SE and BSE signals. Different metals of varying thicknesses were deposited on kidney slices and the SE and BSE images of glomerular endothelial membrane surface were compared with respect to topographic contrasts and resolution at low ($\sim$ 1,000 x), medium (30,000 x) and high (100,000x and 250,000 x) magnifications. Since the metal film was imaged and not the specimen surface, not only surface contrasts but also relevant properties of the metal films affecting the image are discussed, i.e., the ability to enhance the contrast of macromolecular surface fine structures.

Materials and Methods

Microscope.

A JEOL JSM 30 cold field emission microscope was used and operated at 30 kV with a beam diameter of $\sim$1 nm and beam currents of $5\cdot10^{-12}$ - $1\cdot10^{-11}$ A. The images were recorded with 2,000 lines in 50 sec on Polaroid film type 55 and printed without any image processing for noise reduction (Peters, 1985a).

Magnifications are indicated in the micrographs by a scale bar and, in order to facilitate appreciation of small dimensions, are additionally described in the figure legends by a numerical expression.

The stereo micrographs in figures 11 - 15 may be viewed with stereo prisms (System Nesh). The inexpensive plastic prisms were obtained from Balzers High Vac. Corp., Nashua, NH (Part No.: B80 1004 045) or from Marvik Ld., Halifax NS, Canada (Part No.: 0 640).

Specimen for Testing Signal Collection.

Colloidal gold particles, 15-20 nm in diameter, were stabilized with 1% polyethylene glycol (Horrisberger and Rosset, 1977) and mixed with suspensions of tobacco mosaic virus (TMV) and ferritin. The particles were adsorbed to silicon wafer chips, 5 x 7 mm in size, dehydrated in three steps in 30%, 60% and absolute ethanol and air dried. The preparation details were previously described (Peters, 1982b and 1986).

Biological Specimen Preparation.

The biological tissue was perfusion-fixed and prepared for electron microscopy as follows. Under light ether anesthesia, male Swiss albino mice were perfused at constant pressure through the left ventricle with warmed Dulbecco's phosphate buffered saline supplemented with 14 mM glucose (PBSG) at a rate of 3.5 ml/min and a pressure of 60 - 80 mm Hg. The right ventricle was cut open to allow easy outflow of the perfusate. The whole animal was fixed by perfusion in situ with warmed 3% glutaraldehyde in 0.1 M sodium cacodylate buffer, pH 7.2. After fixation for $\sim$10 min, the kidneys were removed, cut into large wedge shaped pieces of 2 x 8 mm in size and immersed in the same fixative for 2 hours at 4°C. Then after rinsing in PBSG, post fixation in veronal acetate buffered 1% OsO_4 (pH 7.6, 4°C) was carried out for 2 hours. After rinsing in PBSG, the kidney pieces were cut with a vibratome into 100 - 150 μm thick slices and additionally fixed for 30 min in the buffered OsO_4. The tissue slices were then treated so as to obtain a "controlled osmium impregnation" (Peters and Green, 1983). One to four slices were washed at 20°C in 45 ml of 0.15 M NaCl under rocking motion 5 times for 10 - 15 min at each time before being treated with thiocarbohydrazide (TCH, saturated in 0.15 M NaCl) for 10 min at 20°C. The specimens were then washed 8 times as above with NaCl and successively immersed in 1% buffered OsO_4 for 10 min at 20°C. After final washing for 4 - 5 times with H_2O the slices were transferred into BEEM containers for dehydration in a continuous gradient between H_2O and absolute ethanol and absolute ethanol and Freon 113 (TF) and critical point-dried in CO_2 according to the exchange method (Peters, 1980a). After drying, the slices were mounted for metal deposition with double stick tape onto silicon chips. Specimens for direct observation without metal application were mounted on chips covered by a thin layer of carbon paste (DAG 154, Acheson Colloids Co., Port Huron, MI). Slices not immediately used were stored in BEEM containers closed by another, second lid.

Metal Deposition.

Metal was deposited onto the mounted specimens by Penning sputtering (Jacopič et al., 1978) in a Balzers BEA 120 vacuum evaporation unit (Peters, 1980b). During deposition the specimens were tumbled with a 0 - 90° tilt- rotating movement (Samspin: Tousimis Res. Corp., Rockville,
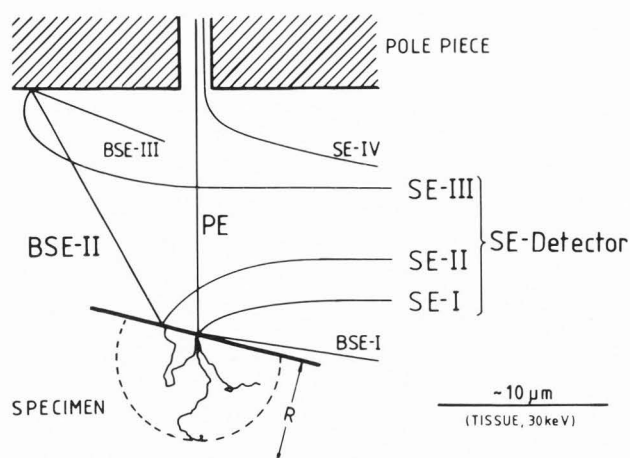
Fig. 1 Types of signals, backscattered (BSE) and secondary electrons (SE), generated by the primary electrons (PE) of the probe in a standard SEM.
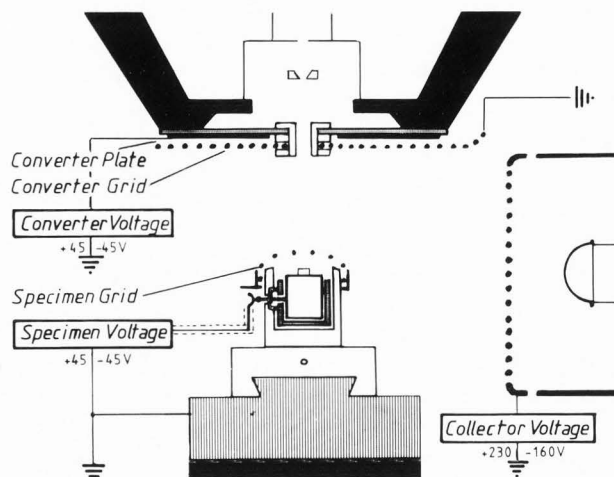

Fig. 2 BSE-to-SE converter used with grounded specimen grid and provided for electrically biased specimen.

MD) and 4 times the amount of metal which actually landed on the specimen surface was deposited onto the specimen plane (deposition factor = 25%; see for details Peters, 1986).

Final Specimen Handling.

After metal deposition the silicon chips were mounted on Al specimen stubs with carbon paste, predegassed at ∿1 Pa for 30 min and degassed at <10^{-5} Pa for 2 hours. The specimens were quickly transferred into the microscope and observed at a vacuum of 10^{-6} Pa.

Signals

High magnification imaging with SE and BSE, generated in very thin metal films, was achieved by applying a special signal collection strategy described in the following. Sufficient signal strength was established by using a high brightness gun and a small beam diameter of ∿1 nm (Peters, 1979). The high resolution signal components are also produced in a conventional microscope operated with a tungsten filament and beam diameters of 3 - 10 nm (Peters, 1982b). However, with such instruments high magnification contrasts may be imaged only in part because they are obscured by other contrasts and high noise levels. The results shown here may be used to improve the imaging to the limits set by a particular conventional instrument. Modern analytical as well as standard microscopes allow significantly improved imaging of high magnification contrasts if they are equipped with LaB_6 or field emission cathodes. It is especially for these microscopes that the imaging strategy is discussed in order to establish a resolution closely related to the beam diameter used.

SE and BSE Signals.

Since BSE and SE are both involved in generating contrasts and in enhancing or reducing topographic resolution, they are characterized here not as a function of the sequence of scattering events in which they are produced (Reimer et al., 1968; Drescher et al., 1970) but

in conjunction with the spatial relation between their point of emission and the site of the electron probe. This slightly altered classification (Peters, 1982a and b; Pawley, 1984) facilitates interpretation of contrasts at medium and high magnifications.

Types of Signal. When they enter the specimen the electrons of the probe, primary electrons (PE), produce three types of electrons which may be collected in a signal (Fig. 1). At the point of incidence and in the first scattering event type I signals are produced. Then, scattered PE may emerge from the specimen at some distance from the point of entry and produce at the specimen surface type II signals or they may leave the specimen and produce at the walls of the microscope chamber type III signals. All electrons generated by PE before reaching the specimen are collectively described as type IV electrons.

The type I signals (BSE-I and SE-I) are the high resolution signals since their excitation volume is most closely located around the site of impact of the PE and extends only a few nm (∿1 - 5 nm) from the surface into the specimen. The exit area on the surface is nearly independent of the acceleration voltage and measures only a few nm in diameter. Because of their low excitation depth the type I signals carry surface information ("real or true" surface information).

The BSE-I are produced in negligible numbers at a normal incidence of the probe. Accordingly, conventional BSE signals contain mainly BSE-II. At low incidence the type I electrons increase in numbers and may be enriched in the BSE signal by using a low take-off angle of the detector (Wells, 1979) or by energy filtering (Wells, 1971). The latter collection technique produces the low (energy) loss signal.

The SE-I generation is only partially characterized (Seiler, 1967; Murata, 1973; Wells, 1974; Joy, 1984). Only on very thin specimens of a few nm thickness the SE-I may dominate. Otherwise, on bulk specimens, the SE-II provide the majority

of the signal. In standard microscopes, SE-III are also collected (Everhart et al., 1959). SE-I may be enriched if the emission of the other SE is suppressed (Peters, 1982a, b and 1984a), i.e., by i) eliminating the type III emission or collection, and ii) reducing type II generation through use of low tilt angles and application of very thin metal films of low-atomic number composition on the specimen surface, if appropriate. Then, the imaging of SE-I contrasts requires an increase of the signal/noise (S/N) ratio through use of high brightness guns, high magnification imaging, small beam diameters and reduction of background signal contrast obtained by using high accelerating voltages.

These stringent imaging requirements, designated as "SE-I imaging mode" (Peters, 1982a and 1984b), indicate that the SE-I signal and their contrasts must be very small. The strength of the SE-I signal is still in question. It was suggested that conventional calculations of SE emission from flat surfaces are too high (Seiler, 1983). Moreover, a postulated 1:1 ratio of SE-I:SE-II (Seiler, 1967; Drescher et al., 1970) could not be confirmed by the results of recent calculations which indicated instead a 1:5 - 10 ratio (Joy, 1984). At high accelerating voltage the emission coefficient for both type I signals was calculated to be similar and of the order of 0.01 - 0.02, i.e., 1-2% of PE generate type I signal electrons (Wells, 1975; Joy, 1984).

The type II signals are most commonly used. Their exit area depends strongly on the scattering of PE. Since SE-II are produced by BSE-II, both signals contain information from the depth interaction of PE. However, the SE-II signal may be modified by local surface interactions at the emerging point of the scattered PE since the exit depth of SE is only ∿1 - 5 nm. BSE escape from a 100 - 10,000 times larger depth depending on the energy of the PE and the mass density of the specimen. The specimen topography may, too, alter type II emission since PE leaving the specimen surface at a low angle may extensively scatter at the specimen surface (Hasselbach and Rieke, 1976).

The contrast contribution of the type II signals to low and medium magnification images is still not established (George and Robinson, 1976, 1977a and b; Pawley, 1984). Two strategies are used to reduce the excitation volume in order to increase surface information and topographic resolution: i) the reduction of PE penetration by lowering the accelerating voltage and ii) for specimens composed of low atomic number elements, the application of films of high atomic number metals; a thickness of the film must be smaller than the range of the PE yet thick enough to generate a sufficient S/N ratio of type II signals. The latter strategy produced very similar BSE and SE (type II) images of specimen covered with gold layers >20 nm, even at higher magnifications (Ong, 1970; Lin and Becker, 1975; Crewe and Lin, 1976; Becker and Sogard, 1979).

Whereas the BSE-II are well characterized and measured (Kanter, 1957, Wells, 1977; Niedrig, 1978), SE-II can only be estimated. The measurement of SE yields is very complex (Kanter, 1961a and b; Drescher et al., 1970) since BSE cannot be suppressed and may add an unknown

background of type III SE. Models for SE-II generation have been proposed (Murata, 1973; George and Robinson, 1977b; Joy, 1984) but results are still missing. However, it was suggested that SE II dominate all SE images (George and Robinson, 1976).

The type III signals are a mirror image of the type II with an additional modification by the surface interaction at the microscope chamber and the collection efficiency of the produced electrons. The BSE-III are not widely used but, in the conventional SE detector (the Everhart-Thornley (E-T) detector), they may produce a signal increase of ∿5% (Everhart et al., 1959; Everhart and Thornley, 1960). In a standard SEM, the SE-III are collected with high efficiency by the electrical collection field of the E-T detector and contribute 30 - 60% to the conventional SE signal (Everhart et al., 1959; Seiler, 1967 and 1983; Moncrieff and Barker, 1978; Moll et al., 1978 and 1979; Peters, 1982b and 1984a). The type III component can be effectively eliminated or enhanced by instrumental modifications. In a standard microscope, either a BSE adsorption plate with low emission coefficients for SE and BSE (Peters, 1982a) or an electrically charged plate which is shielded from the E-T detector by a grounded mesh (Reimer and Volbert, 1979) is placed beneath the pole piece. However, SE-III can be used as a "converted" BSE signal (Moll et al., 1978). This concept is also applied here. In an analytical microscope, the specimen is positioned in the last probe forming lens and the E-T detector is placed above the lens (Koike et al., 1971; Kawamoto et al., 1984). It is proposed that for this detector arrangement the electromagnetic collection field excludes a SE-III collection.

Signal Detection. The SE signals were collected with a standard E-T detector (Fig. 2) using a modified BSE-to-SE converter (Reimer and Volbert, 1979). The SE-III component of the signal was generated in part with a converter plate mounted beneath the pole piece. The plate consisted of an electrically insulated copper disk smoked with Mg_2O and shielded from specimen and detector with a grounded Al grid. The plate could be biased negatively or positively by application of a converter voltage in order to release or retain SE-III. The suppression of SE-III allowed a collection of the specimen-specific SE signals only if the specimen was not covered by a specimen grid. Additionally, the specimen was electrically insulated and could by grounded, positively or negatively biased by application of a specimen voltage. In some cases an electrical potential of the specimen made possible an improved SE collection efficiency (Boyde and Cowham, 1980).

At low magnification, a positive specimen voltage may be used to reduce SE collection from the specimen and to enrich selectively the signal with SE-III so as to collect a converted BSE signal (Moll et al., 1978; Boyde and Cowham, 1980). However, this signal is not suitable for high magnifications since it may still contain specimen specific SE (fast SE: Joy, 1984) and since SE-III may be collected with reduced efficiency. Using a converter for an effective SE-III production, the specimen was biased

positively and covered with a grounded specimen grid. This arrangement varies slightly from the BSE-to-SE converter in which the specimen is grounded and the specimen grid is charged. At high magnification, the electrical grid field may reduce the collection efficiency for SE.

The BSE signal, produced at the converter plate, increased when a specimen grid was used since the grid added ∿20% strength to the signal. However, the grid reduced the collection of specimen-specific SE by 50% if the specimen or the grid was appropriately charged. The SE-signal collected from the specimen (Volbert and Reimer, 1980) had a similar composition as the conventional SE signal collected without the converter in the standard microscope: it contained ∿50% SE-III. Another disadvantage of the converter was that the plate saturated already at low BSE doses. Higher BSE loads produced strong local charging of the oxide crystals and the electrical fields penetrated through the grid and affected the beam position at high magnifications. Thus, BSE imaging of bulk metals is a possibility of only limited use.

The converted BSE signal is different from other BSE signals collected by semiconductor or fluorescence detectors because it also contains the low energy BSE component. However, for low BSE signal detection the converter is especially suited because of its low noise (Baumann and Reimer, 1981) and high collection efficiency.

Test Specimen for High Resolution Signal Collection. When using a specimen grid, special care had to be taken to separate SE-(I+II) from SE-III and vice versa. A qualitative and quantitative procedure for specimen-specific signal collection at high magnifications was developed and is described in the following.

Small particles which generate specific and different contrasts for each signal type were adsorbed on carbon films or silicon (Si) wafer chips (Fig. 3). Tobacco mosaic virus (TMV) was very suited since it is small, rod-like and composed only of organic matter. After drying it is ∿16 nm wide (Fig. 3a). The virus particle produced only a weak SE-I edge brightness contrast at its circumference. Due to its shape, the signal may be identified even at a low S/N ratio (Fig. 3b). Ferritin was used as a particle, composed of organic and inorganic matter. It is an iron storage protein and consists of a protein shell, which after drying is ∿11 nm in diameter, and a core of 7.5 nm in diameter which contains variable amounts of iron. The protein shell produced such a weak SE-I signal that it was imaged only on a carbon background (Peters, 1979). The iron core generated a combination of SE-II particle contrast and SE-I material contrast. Most of the SE-I produced in the core were probably adsorbed by the protein shell. As an additional inorganic particle, colloidal gold with particles 15 - 20 nm in diameter was chosen, coated with a thin layer of polyethylene glycol. The gold particles were imaged with a material contrast and a topographic contrast. A SE-I edge brightness of 2 - 3 nm in width (SE range + beam diameter) and a SE-II particle plus SE-I material contrast produced a very strong SE contrast (Fig. 3c). These contrasts could not be distinguished at

Table 1: Useful Magnifications

Feature Sizes	Pixel Sizes	
	0.2 mm	0.5 mm
1 nm	200,000 x	500,000 x
2 nm	100,000 x	250,000 x
5 nm	40,000 x	100,000 x
10 nm	20,000 x	50,000 x
20 nm	10,000 x	25,000 x
100 nm	2,000 x	5,000 x
200 nm	1,000 x	2,500 x
1,000 nm	200 x	500 x

medium magnification (Fig. 3d) but were easily identifiable at high magnifications (Fig. 3e).

Although BSE were produced in all particles only the gold particles generated a signal sufficient for detection (Fig. 3f). The particles were imaged with fading contrast towards their circumferences indicating a weak BSE-II thickness contrast. No edge brightness of a BSE-I signal was imaged. The gold particles were very suitable to assess the collection specificity of the converter for SE and BSE since the SE signal was much stronger than the BSE signal. Traces of a SE signal in the BSE image would have changed the contrast at the particle's circumference and would have imaged also at least the ferritin cores. On the other hand, a SE-I generation and collection was proven with a thin bright contrast outlining the gold particles. High SE-(I+II) collection efficiency was also indicated when the TMV and the ferritin cores were imaged. Since gold and ferritin particles and Si chips are easily prepared, such particulate specimens are convenient and suitable as standard tests to analyze specificity and efficiency of type I signal collection.

Useful Magnifications.
In order to visualize contrasts produced by the type I signals, high magnifications are necessary. The range of SE in gold is ∿1 - 2 nm. If beam diameters of ∿1 nm are used, the edge brightness of a SE-I contrast is imaged as a 2 - 3 nm wide line (Fig. 3c). Such small dimensions cannot be visualized at 37,000 x (Fig. 3d) but they are easily identified at 250,000 x (Fig. 3e).

The magnification at which a smallest visible element of the image (pixel) represents a smallest resolvable detail of the specimen is defined as "useful magnification" (Everhart et al., 1959). To recognize a 2 nm particle with an unaided eye the image must be enlarged to a size of 0.2 mm which requires a magnification of 100,000 x (Siegel, 1964). A further enlargement by a factor 2.5 facilitates the particle recognition; thus, high magnifications are required to image type I signal contrasts. Table 1 summarizes useful magnifications for different feature sizes of specimens.

Contrasts

Contrasts produced by the specimen's structure are well defined for low and high magnification on bulk and metal coated specimens
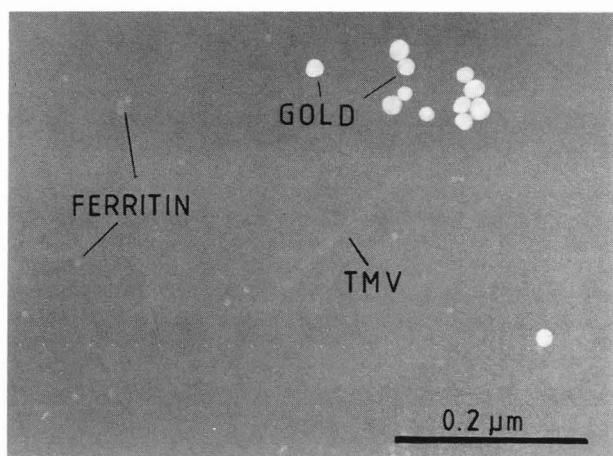
Fig. 3a Test specimen for type I signal collection at high magnification. Ferritin, tobacco mosaic virus (TMV) and colloidal gold on carbon film in TEM. (x 125,000).
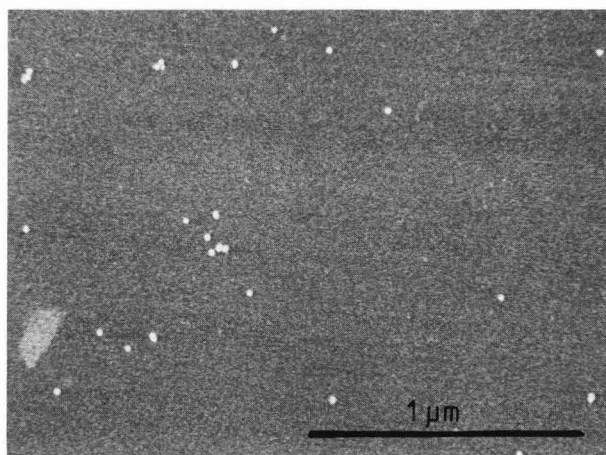

Fig. 3d Medium magnification image of the test specimen. Signal type I contrasts, i.e., TMV particle contrast or SE-I edge brightness contrast on gold particles, are not detected. (x 37,000).
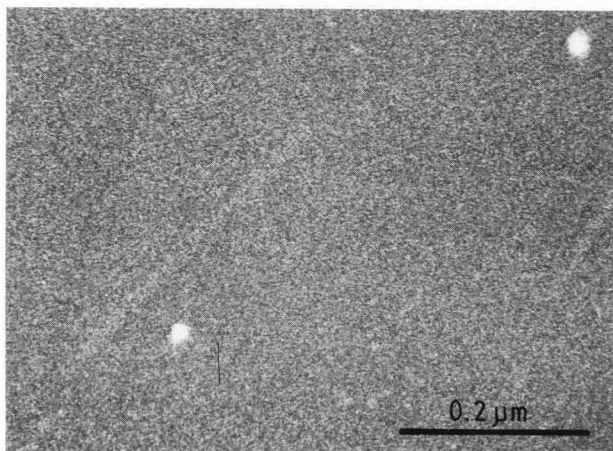

Fig. 3b The same test specimen on thin carbon film in SEM. Only very little background signal (∿5% of total specimen specific SE signal) is generated. (x 125,000).
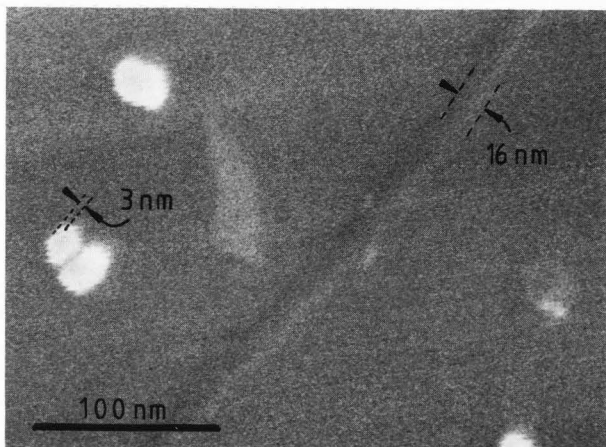
Fig. 3e High magnification SE image. SE-I edge brightness is high on gold particles but low on TMV and not efficiently collected from sides opposite to the detector. (x 250,000).
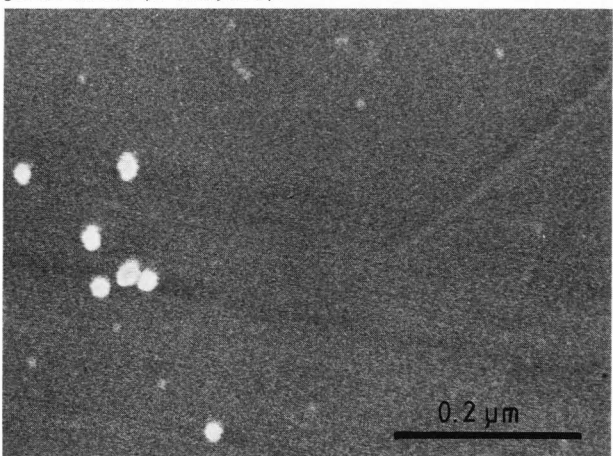
Fig. 3c Test specimen on bulk silicon chip in SEM. Note thin bright contour on gold particles produced by SE-I as edge brightness contrast. (x 125,000).
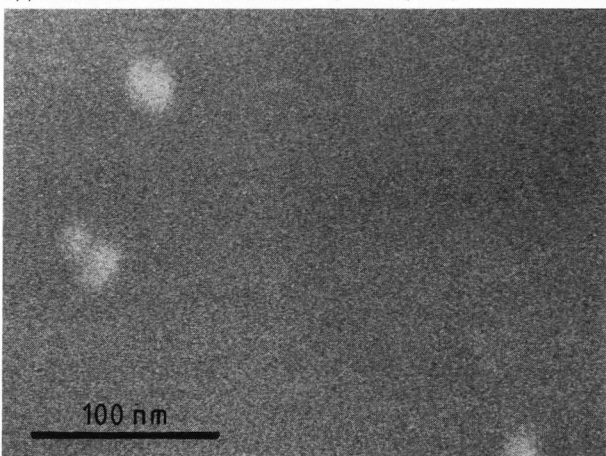

Fig. 3f High magnification BSE image of the same area as seen in figure 3e. Only the gold particles generate a sufficient BSE particle contrast. No type I signal contrast is imaged. (x 250,000).

To facilitate comparison of figures (of identical magnification or of other published results) magnifications are indicated by numerals placed at the end of each figure legend.

(Wells et al., 1974). Two kinds of contrasts are produced on a surface: i) if the material varies, material contrasts are generated, and ii) if the incident angle of the beam on the surface varies, topographic contrasts are generated. Additionally, signal collection mechanisms alter the contrast significantly. Collection efficiency contrasts are most common and depend on the position of the signal detectors in relation to the specimen. In a SE image this phenomenon produces shadows behind features in the direction opposite to the detector (Figs. 3c and e) and adds an important contrast to the standard microscope, since ~50% of the SE, emitted from the surface, are collected (Reimer, 1978). This type of contrast is very much reduced in an analytical microscope. In standard microscopes, two SE detectors may be used to reduce collection efficency contrasts (Volbert and Reimer, 1980). However, voltage contrasts and charging artifacts may be observed in both kinds of instruments on specimens of low electrical conductivity.

Voltage contrasts are also a result of an increase or a reduction of the signal collection efficiency, but in this case caused by specimen specific phenomena of charging, i.e., accumulation of electrical charges in the specimen. This causes an uneven, spotty appearance of low magnification images. Internal electrical fields may be so strong that the electron probe is deflected or that electrons are emitted from the specimen. These phenomena cause charging artifacts. In conventional microscopy, these contrast mechanisms are reduced if thick metal films are applied which backscatter the PE to such an extent that electrons do not accumulate. For high resolution microscopy with thin metal film application, a floating voltage technique may be used (Peters, 1979). However, it is easier to increase the specimen's electrical conductivity by a controlled osmium impregnation (Peters and Green, 1983). Then high accelerating voltages can be used to increase PE penetration and distribution into a larger specimen volume.

Topographic High Magnification Contrasts.

Topographic contrasts depend on the dimension (d) of the specimen feature and on the radius of the exit area of the signal (Peters, 1984b). The radius is approximately equal to the range of PE, in the case of type II signals, or to the range of type I signals. In order to facilitate the interpretation of contrast phenomena it is assumed that range (R) and radius of exit area are of equal dimensions. If R<d, strong edge brightness contrasts but weak relief contrasts are produced. If R>d, two other contrasts are generated depending on the smallest resolvable dimension (r). If R>d>r, electrons emit on the whole surface of the feature and a particle contrast is produced. However, if R>d<r, the particles are not resolved but an increased number of electrons are emitted from the increased surface area causing a weak micro-roughness contrast.

Use of Metal Films for Contrast Generation.

Topographic resolution on bulk specimen may be increased if metal films thinner then R are used (Ong, 1970; Everhart and Chung, 1972). If thin metal films are applied, both the film and the specimen contribute to the signal. The specimen contributes the background signal which carries useful information only at low magnifications. At high magnification contrasts are generated predominately by the metal film. For type I signals mainly a thickness contrast is produced which is equal to the length the PE have to travel through the metal. Very weak relief contrasts but very strong contrast at edges are produced. At particles (d>r) the contrast at the circumference is similar to the contrast at the edges. On flat surfaces only weak micro-roughness contrast is expected (d<r) and is found mostly on the level of the substructures of the metal film. However, on convoluted surfaces and if the metal substructure is very coarse, as in discontinuous films, the micro-roughness contrast may be larger than other type I contrasts and thus reduce resolution. This effect on high magnification contrasts is demonstrated in the following.

Results and Interpretations

The imaging of macromolecular surface fine structures on biological specimens is only possible with a high resolution type I signal and requires contrast enhancement with metal films. In the SE-I imaging mode, a specimen-specific signal of SE-I and SE-II [SE-(I+II)] is used to image the SE-I contrast of features a few nm thin or high and wide. For that signal, SE-II contribute a background component that may obscure the SE-I contrasts. To decrease this component and to increase SE-I/SE-II ratio, i) the film thickness was reduced, ii) the metal film continuity and homogeneity was improved, iii) metals of low SE-II emission were chosen, and iv) the osmium impregnation was held to the minimal amount necessary to prevent specimen charging.

Since SE-II contributes the major signal component, its contrast contribution was assessed by imaging the BSE signal from identical areas. Since the BSE are mainly of the type II it is possible to estimate the relative proportion of SE-II contrast contribution to the SE-(I+II) signal.

On kidney slices, glomeruli were imaged at low magnifications (~1,000 x) and the luminal surface of the glomerular fenestrated capillary endothelium was imaged at medium (30,000 x) and high magnifications (100,000 x and in stereoscopic images at 250,000 x).

Uncoated Biological Specimens.

The kidney slices were impregnated with osmium black (Hanker et al., 1964) in such a manner that the exposed cell surfaces were free of any precipitation. Thus, OTO-coating (Kelley et al., 1973) was strictly prevented (Peters and Green, 1983). In order to assess the contrasts produced by metal application the cell surfaces were first imaged without a metal layer.

SE Contrasts. Such Os-impregnated but not metal-coated kidney slices were easily imaged in the SE mode. Little voltage contrast was recognizable at low magnifications (Fig. 4a - asterisk). Glomerular capillary walls and tubule walls were imaged only in particle contrasts; edge brightness contrasts were barely recognizable. At medium magnifications (Fig. 4b) on a small portion of an endothelial cell luminal surface (referred
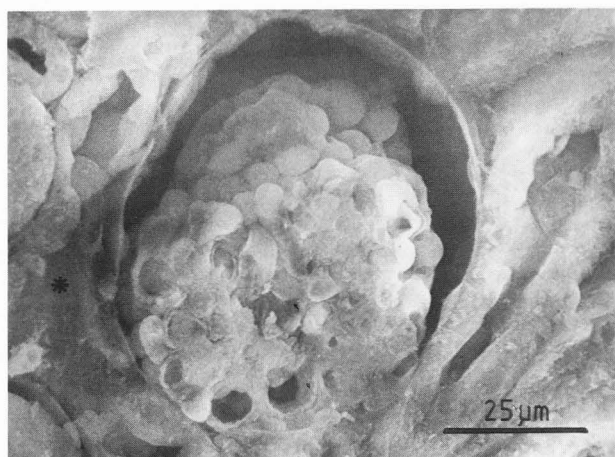
Fig. 4a SE image of a biological specimen after osmium impregnation but without any metal coating. Weak edge brightness and little detail are detected. (x ∿1,000).
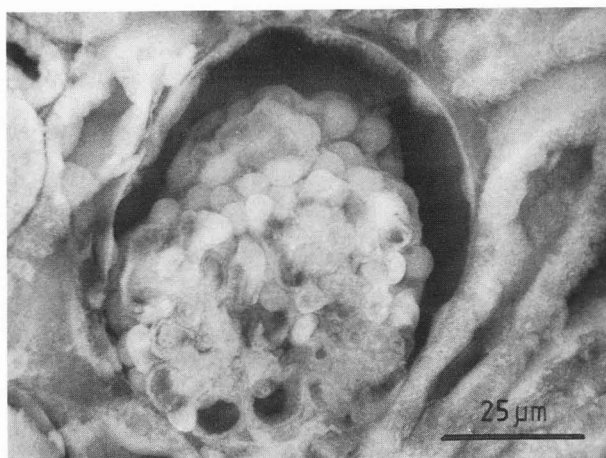

Fig. 4d BSE image of same specimen imaged in figure 4a. Very similar contrasts as in the SE image indicating similar excitation area for both signals. (x ∿1,000).
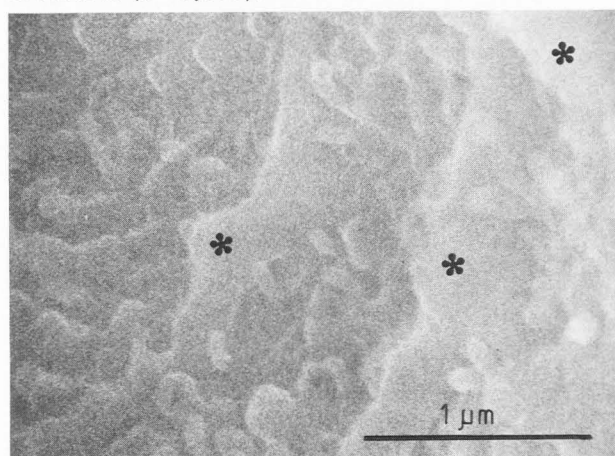

Fig. 4b SE image at medium magnification. Few and weak contrasts with a low signal/noise (S/N) level are recored. SE-II particle contrasts (asterisks) dominate. (x 30,000).
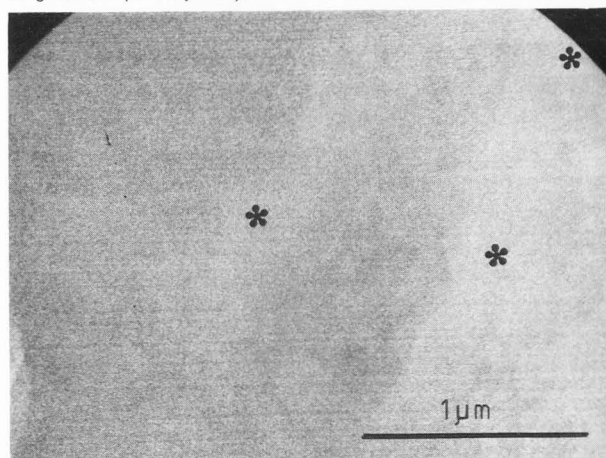

Fig. 4e BSE image at medium magnification. Only very weak particle contrasts (asterisks) are recognizable but no edge brightness contrasts are apparent. (x 30,000).
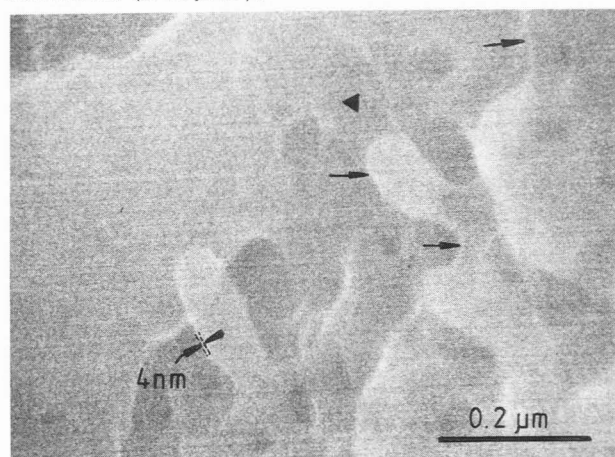
Fig. 4c SE image at high magnification. S/N ratio is improved when compared with figure 4b. Now, the SE-I edge brightness contrast (arrows) is dominant. (x 100,000).
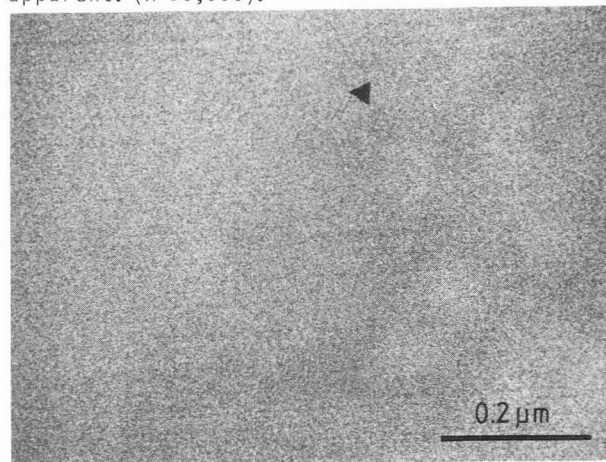

Fig. 4f BSE image at high magnification. Low S/N ratio excludes sufficient imaging of defined feature contours. Background signal strength is low in the dark area (triangle). (x 100,000).

to hereafter generally as cell surface), the SE signal revealed a low S/N ratio. However, two distinct contrasts were imaged. Microvilli and cytoplasmic ridges were bright and seen in particle contrast (asterisks) and were outlined by a weak but recognizable thin line.

At high magnifications (Fig. 4c) the S/N ratio improved and both contrast types were more clearly imaged. The bright sharp lines were ⅃4 nm in width and outlined all elevated features. This contrast was a SE-I edge brightness contrast. No other SE-I contrasts, i.e., relief and particle contrasts, were obvious. However, very weak, small, fuzzy dots of >10 nm were barely visible on the cell surface. All elevated features revealed an SE-II particle contrast of constant level over their entire surfaces.

BSE Signal Contribution. The strength of the BSE signal was equal to that of the SE signal and gave, at low magnifications (Fig. 4d), a very similar image. Voltage contrasts were absent as well as an edge brightness. This lack of edge effects was confirmed at medium magnifications (Fig. 4e). Barely identifiable were cytoplasmic ridges and microvilli imaged in weak particle contrast. At high magnification (Fig. 4f), the S/N ratio decreased so much that feature contours were no longer defined. This was just the opposite of the SE-I S/N ratio which improved at high magnifications.

Comparison of SE and BSE contrasts. On surface areas which generated the lowest BSE signal (Fig. 4f - triangle), SE-II production must have been minimal and thus these areas should reveal an enriched SE-I signal in the corresponding SE image (Fig. 4c - triangle). Compared with the background signal seen over the fenestrae, the low SE-I signal reveals a weak SE-I material contrast component of the tissue. Obvious contrasts originate in part from SE-I (edge brightness) and in part from SE-II (particle contrast). However, at high magnifications the image was dominated by the bright contours of the SE-I contribution.

Specimens Decorated with Thick Continuous Metal Films.
Conventionally, biological specimens are coated with 10 - 20 nm thick metal films (Echlin, 1972) to increase electrical conductivity and surface contrasts.

SE Contrasts. In fact, after applying an even 10 nm thick gold film, a crisp image full of small surface details (>200 nm, see table 1) was imaged at low magnifications (Fig. 5a). Edge contouring was increased, but glomerular capillary and tubule walls showed particle contrast similar to those found in specimens not coated with metals. At medium magnifications (Fig. 5b) the capillary surface was imaged with good S/N ratio as smooth areas which revealed some details at high magnification (Fig. 5c). The fenestrae were contoured by bright lines (arrows) and the metal surface was covered with bright spots of 2 - 5 nm in size. These fine structures are small gold crystals grown on the surface of the continuous metal film.

BSE Contrasts. The BSE image (mainly contributed by BSE-II) differed only at low magnifications (Fig. 5d) from the SE images. Low

contrasts and lack of edge contouring were very similar to BSE images of uncoated specimens (Fig. 4d). The BSE image improved at higher magnifications and revealed very similar contrast as the SE images. However, the S/N ratio was somewhat lower although the total BSE signal strength was ⅃50% higher than that of the SE signal. Doubling the signal collection time of the BSE would have made both signals identical. At medium (Fig. 5e) and high magnifications (Fig. 5f) all contrasts seen in the SE image were also seen in the BSE image, especially the width of the bright outlining of the cell body. In some areas of the image even a small substructure of the metal films was imaged by the BSE-II although with low S/N ratio. Fuzzy disks of ⅃10 nm in diameter were contoured by ⅃2 nm wide dark lines and indicated subsurface mass density variations of the gold layer.

Comparison of SE and BSE Contrasts. The differences between the SE and BSE contrasts at low magnification and the similarities of contrasts at higher magnifications revealed a basic and important phenomenon encountered when working at higher magnifications on specimens covered by a thick metal layer. At low magnifications only large specimen features were imaged and the contrasts were strongly dependent on penetration distance of the primary electrons and on the size of the features. The low contrasts, produced at 30 kV accelerating voltage by BSE (Fig. 5d), indicated a large range of PE. The range of the PE was reduced by lowering the accelerating voltage. At 25 kV (Fig. 5g) the particle contrast of the tubules or capillaries was reduced and additional small structures were imaged. At 15 kV (Fig. 5h) the particle contrast was almost reduced to an edge contour and at 8 kV (Fig. 5i) it disappeared leaving a very flat contrast of larger features but increased contrast of the smaller details.

When compared with the SE image generated with 30 keV PE (Fig. 5a), contrasts of the BSE image produced with 25 keV PE (Fig. 5g) were very similar, irrespective of the difference in exit area of each signal. At low magnifications the SE signal of each pixel was produced from a smaller surface area than the BSE signal. This can explain the difference in contrasts between the SE and BSE images at the same accelerating voltage. However, at high magnifications, this difference did not influence the contrasts because it contributed now only to the background signal. In this case, imaged contrasts were produced in a much smaller excitation volume which was identical for both (SE and BSE) signals, as documented in the identical width of the edge contours (Figs. 5c and f - arrows). These findings indicated that all contrasts imaged with SE were produced by a type II signal generated by BSE. The width of the contours is 4 - 10 nm. Since the SE-I range in gold is ⅃1 nm an edge brightness of 2 - 3 nm is expected on a bulk sample (Peters, 1984a). Some contours were indeed imaged with such a width but the contrast was very low. Thus, nearly all contrasts seen at high magnifications were produced by type II electrons, i.e. edge brightness and particle contrast and a strong material contrast (cell surface versus fenestrae).
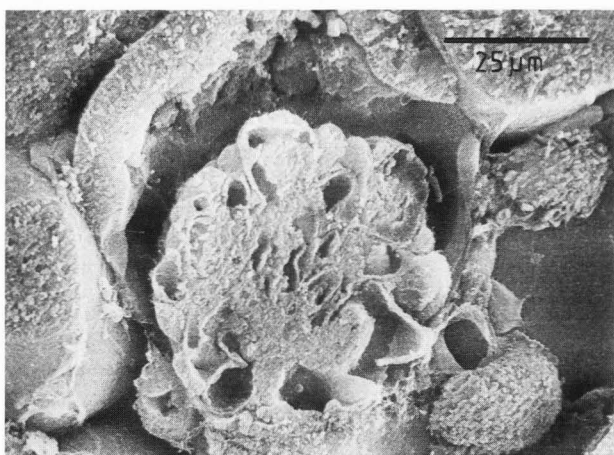
Fig. 5a Biological specimen decorated with a 10 nm thick gold film by tumbling deposition. The SE image is rich in details. The smallest features identifiable are 100 - 200 nm in size. (x ∿1,000).
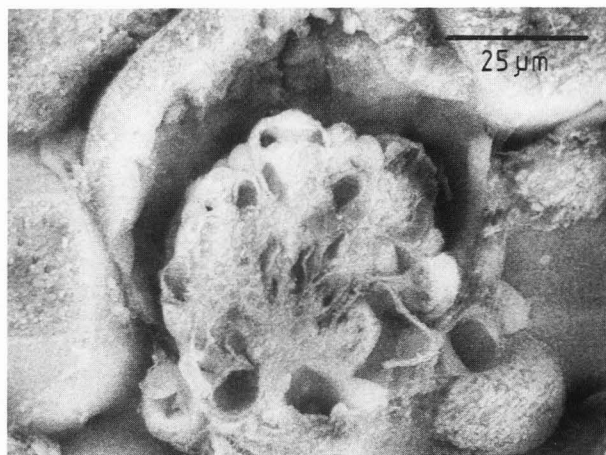

Fig. 5d BSE image (30 keV PE) of the specimen imaged in figure 5a. The constrasts are weaker than in the SE image. Edge contouring and details are lacking. (x ∿1,000).

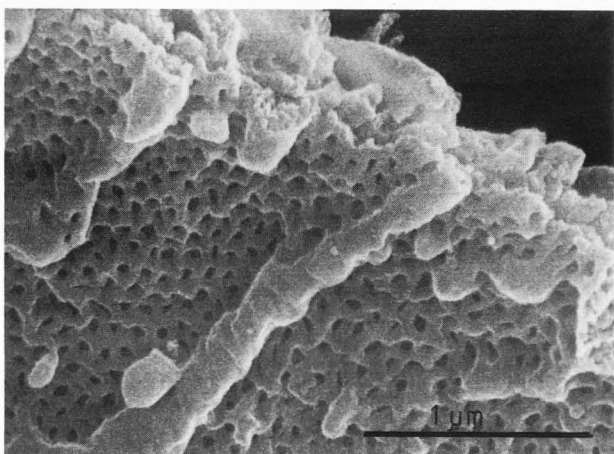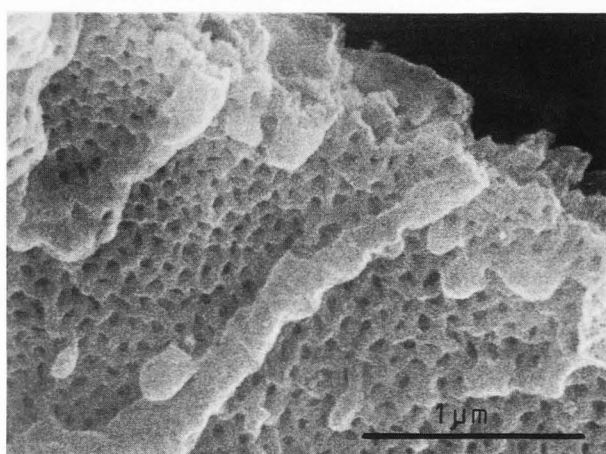Fig. 5b SE image at medium magnification. Good S/N ratio of the SE-II signal. No SE-I signal is detected. (x 30,000).

Fig. 5e BSE image at medium magnification. Good contrast identical with SE contrast imaged at the same magnification. Compare with figure 5b. S/N ratio is somewhat lower. (x 30,000).
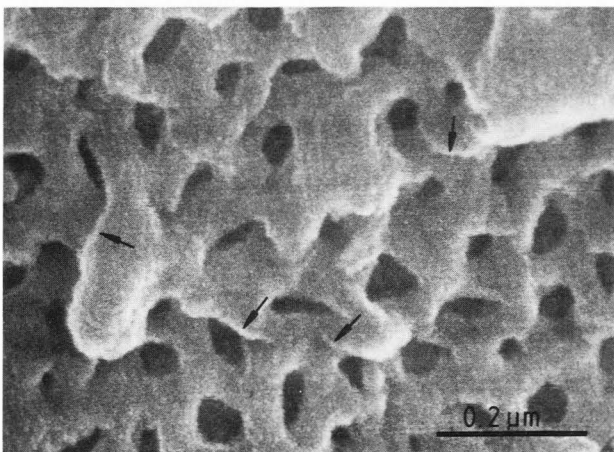

Fig. 5c SE image at high magnification. No biological surface details are imaged. The smallest details are produced by gold. Edges are contoured by SE-II contrast. (x 100,000).
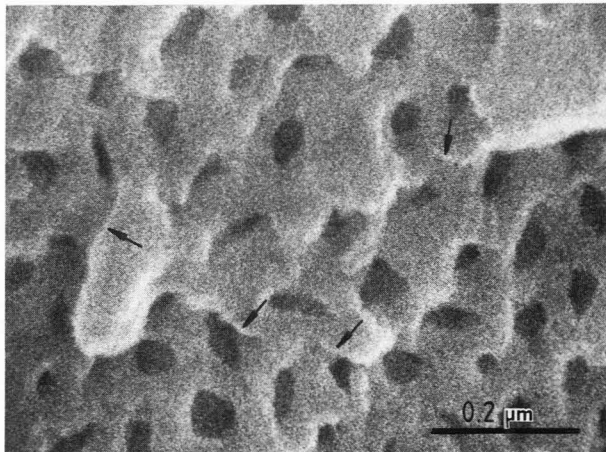

Fig. 5f BSE image at high magnification. All contrasts imaged by SE (see figure 5c) are also imaged by BSE. This proves that all SE contrasts are produced by a type II signal. (x 100,000).
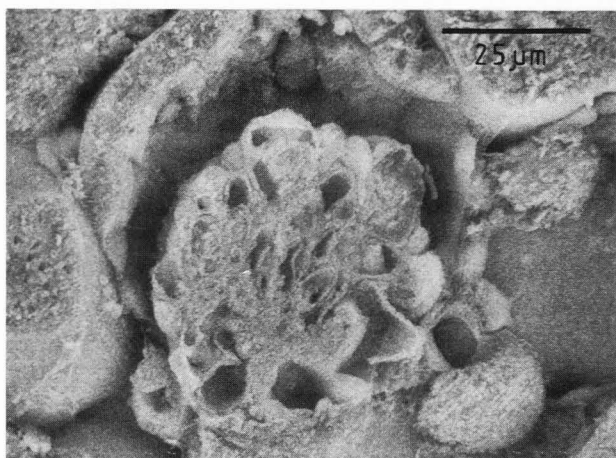
Fig. 5g BSE image produced by 25 keV PE. Similar contrasts as seen in the SE image in figure 5a. This indicates larger signal excitation area for BSE than SE at identical keV. (x ∿1,000).
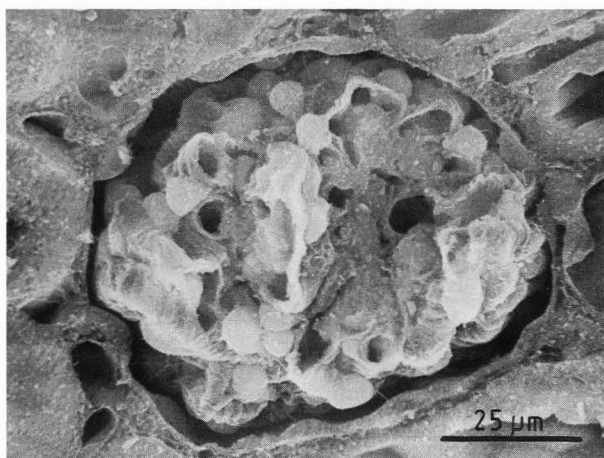

Fig. 6a Specimen decorated with a discontinuous 5 nm thick gold film. The SE image at low magnification shows good contrasts of large and small features. (x ∿1,000).
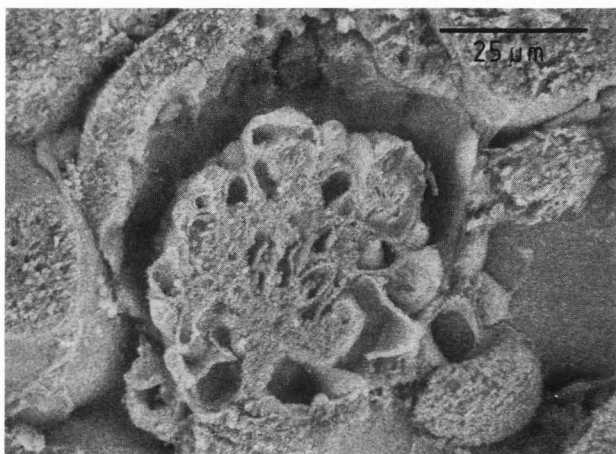

Fig. 5h BSE image produced by 15 keV PE. Increase of edge contouring of small particles makes the image richer in contrast when compared with that in figure 5g. (x ∿1,000).
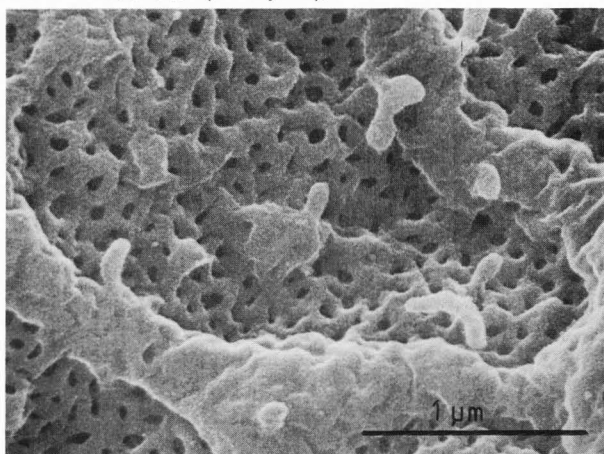

Fig. 6b SE image at medium magnification. The contrasts obtained are very similar with those generated by a 10 nm thick decoration (figure 5b). Sufficient S/N level. (x 30,000).
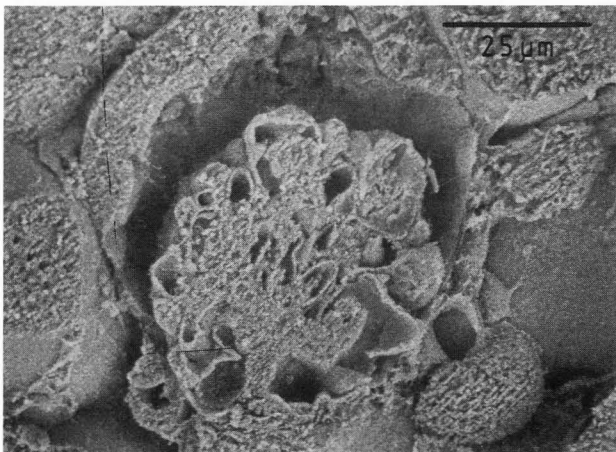

Fig. 5i BSE image produced by 8 keV PE. Signal generation area imaged only by a few pixels: this increases particle contrast and diminishes the edge brightness of large features. (x ∿1,000).
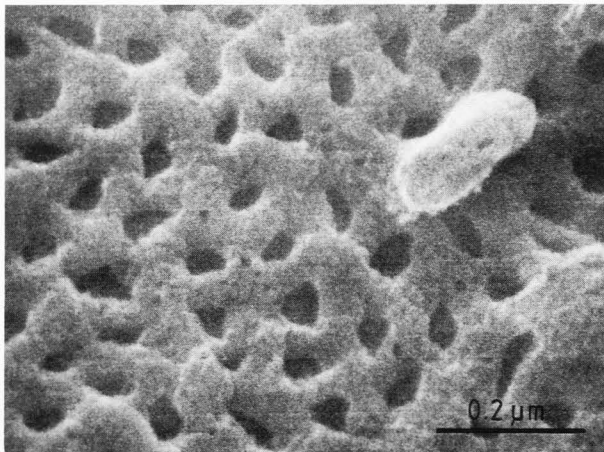

Fig. 6c SE image at high magnification. Contrasts at low S/N level reveal closely packed round disk-like gold structures. Occasional holes indicate that a few particles are missing. (x 100,000).
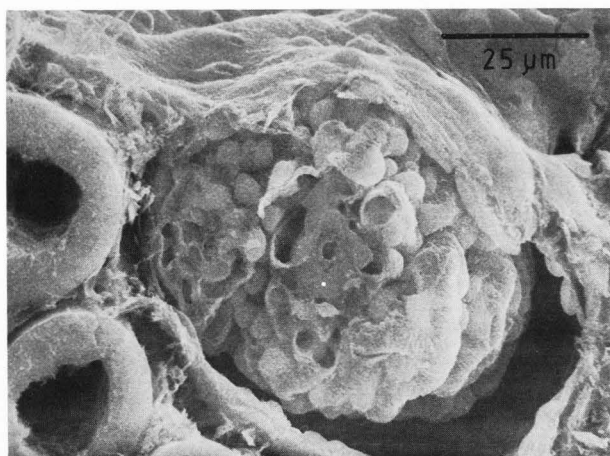
Fig. 7a Specimen decorated with a 1 - 2 nm thin discontinuous layer of gold. The SE image shows only low contrasts similar to those recorded as an uncoated specimen (figure 4a). (x ∿1,000).
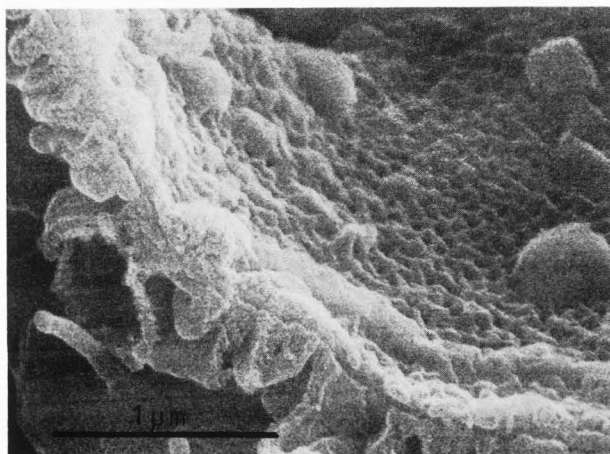

Fig. 7b SE image at medium magnification. The image shows mostly SE-II contrasts at a low S/N ratio. Edge contouring at the fracture plane includes some type I signal contrast. (x 30,000).
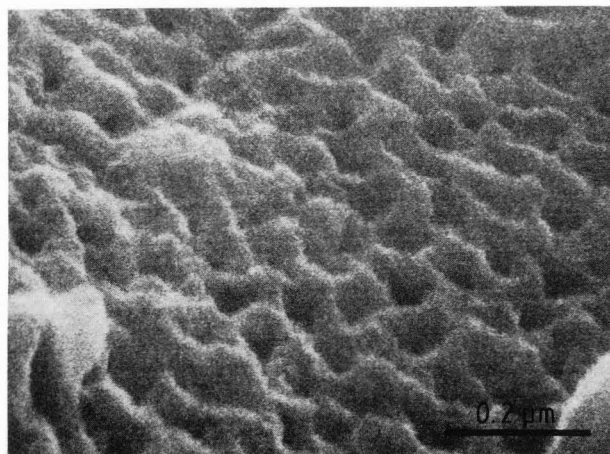

Fig. 7d SE image at high magnification. Only very weak small spots are recognizable on the cell surface, but stronger contrast contours the fenestral rims. (x 100,000).

The thick metal coating obscured the SE-I contrasts and also covered all surface fine structures.

Specimens Decorated With Thin Discontinuous Metal Films.

Resolution can be improved with thinner metal films on two accounts: i) fine structures are not blanketed by metal, and ii) the SE-I/SE-II ratio is improved since the signal excitation volume gets smaller and less BSE-II are produced. SE-I contrasts may become visible if the S/N ratio is sufficiently high. However, at higher magnifications the size and distribution of the metal atom clusters in the film become a dominant factor in the generation of signal and image contrasts.

If the thickness of the gold films was reduced below 10 nm, the films became discontinuous and strong decoration effects of the macromolecular fine structure of the cell surfaces became an important image element. Additionally, the S/N ratio decreased.
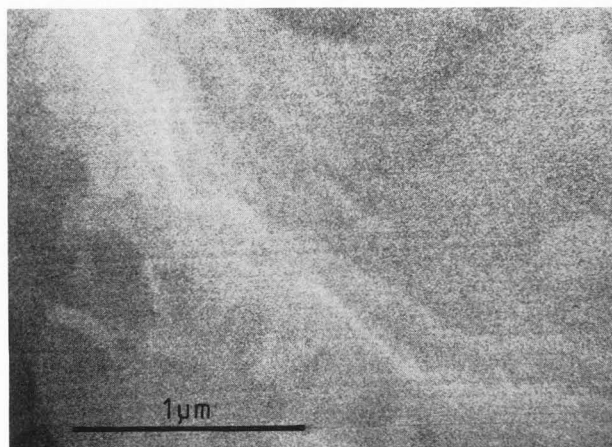

Fig. 7c BSE image at medium magnification from the area imaged in figure 7b. Most contrasts seen in the SE image (figure 7b) are generated by BSE, except edge contouring. (x 30,000).

5 nm Thick Gold Decoration. At low magnification (Fig. 6a), the SE contrasts were quite similar to those obtained from a 10 nm thick continuous gold film. The signal also imaged the cell surface with a good contrast at medium magnification (Fig. 6b). However, at high magnification (Fig. 6c) the S/N ratio decreased.

The metal layer was composed of 10 - 15 nm large patches of metal aggregates which were closely packed on the cell surface. Some missing patches left holes of similar sizes in the metal film. The metal accumulations showed some finer substructures which seemed in part outlined by a low edge contrast. The fenestrae were always contoured by a wide edge brightness. The discontinuities in the metal layer were very distracting and the image revealed an increased noise level caused by micro-roughness effects in the metal film.

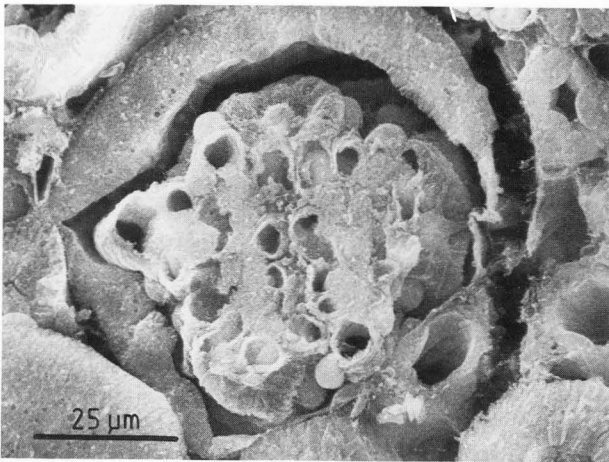1 - 2 nm Thick Gold Decoration. Very thin gold films were discontinuous and produced only

Fig. 8a   Specimen decorated with a discontinuous 1-2 nm thick platinum film. The SE image at low magnification indicates good contrasts. (x ∿1,000).

little contrast and much background noise. At low magnification (Fig. 7a) the glomerulus was only imaged with weak SE contrasts similar to an uncoated specimen (see Fig. 4a). At higher magnifications the image was very noisy (Fig. 7b) and only little BSE contrast was produced (Fig. 7c). However, all details of the SE image could be recognized in the BSE image, including the fenestrae. This indicated the presence of a high type II signal component in the SE image. At high magnification (Fig. 7d) .only very weak fuzzy spots were imaged on the cell surface with a similar distance to each other as the round patches imaged in figure 6c. The fenestrae were outlined with sharp contours. This lack of surface detail is surprising because individual gold accumulations were expected to produce a strong SE signal due to their height of several nm. Obviously, a high background noise, generated by the discontinuous film, had deteriorated the surface contrasts.

1 - 2 nm Thick Platinum Decoration.   The platinum film had a much finer substructure than the gold film and was nearly continuous (Peters, 1982b). It produced good contrasts at low (Fig. 8a) and medium magnifications (Fig. 8b) equal to those of a 5 nm thick gold film. However, at high magnification (Fig. 8c) the cell surface is more evenly covered when compared with the gold decoration (see Fig. 6c). No obvious discontinuities were imaged and the recognizable substructures had the same spacings as those seen in the gold layer. The surface is similar to that seen after a 10 nm gold decoration (Fig. 5c). Additionally, very fine bright edge contouring of the fenestrae occurred. By comparison, the BSE image showed strong material contrast at high magnification (Fig. 8d). In certain areas of the BSE image, very small discontinuities around the film substructures were recognizable. However, in most cases no equivalency to the intensity of edge brightness in the SE image was seen. This was contrary to the edge brightness produced in thick gold films (see Figs. 5c and f). Although most of the cell surface was imaged by SE-II, a
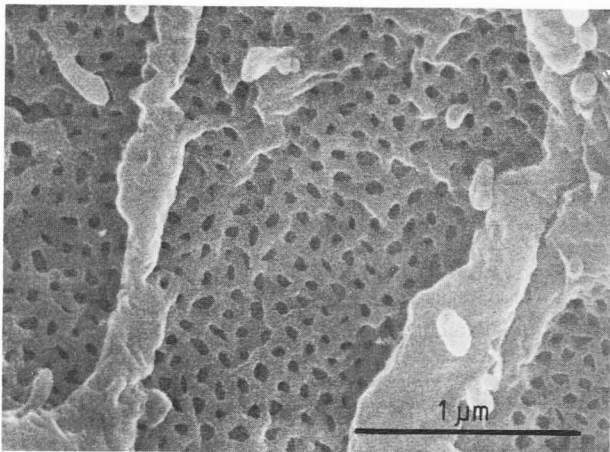

Fig. 8b   SE image at medium magnification. The image contrast is equal to that given by a 5 nm thick gold decoration. Additionally a very fine edge contouring is recognizable. (x 30,000).
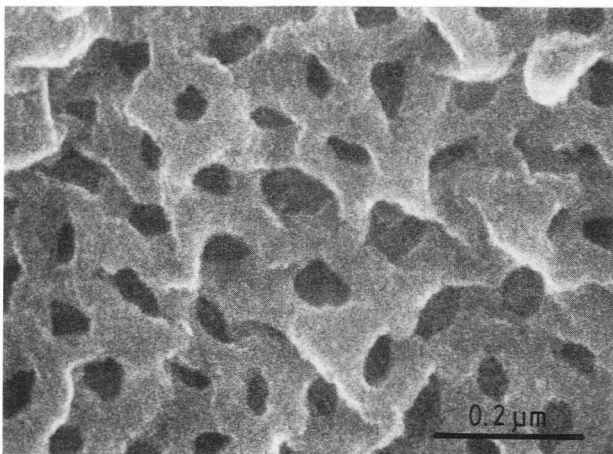

Fig. 8c   SE image at high magnification. The cell surface is imaged with uniform contrast and small fuzzy spots. Very fine SE-I edge brightness is recognizable. (x 100,000).
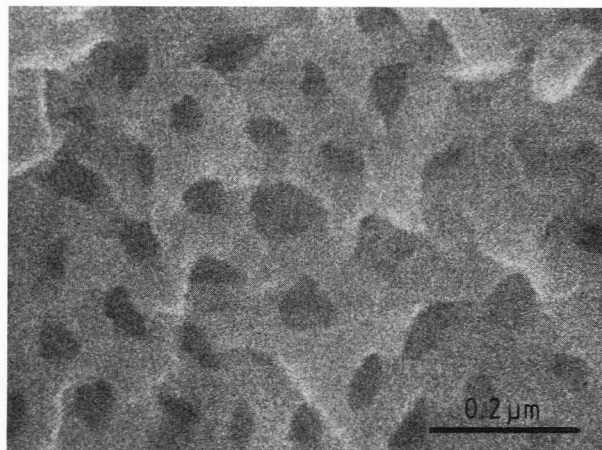

Fig. 8d   BSE image at high magnification from the same area as imaged in figure 8c. Strong material contrast but only very weak topographic contrasts are detected. (x 100,000).
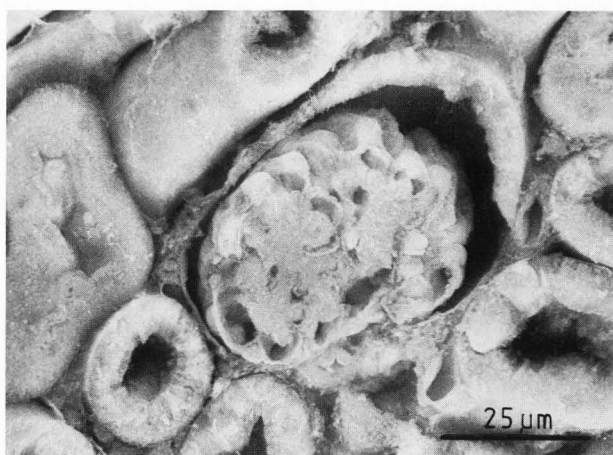
Fig. 9a Specimen coated with a 5 nm thick continuous tantalum film. The low magnification SE image lacks edge contouring and detail indicating a large signal excitation volume. (x ∿1,000).
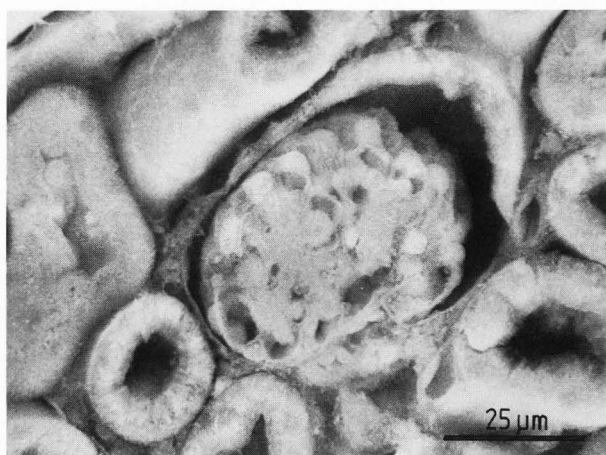
Fig. 9d BSE image of the specimen shown in figure 9a. The low magnification image shows similarly weak contrasts as does the corresponding SE image. (x ∿1,000).
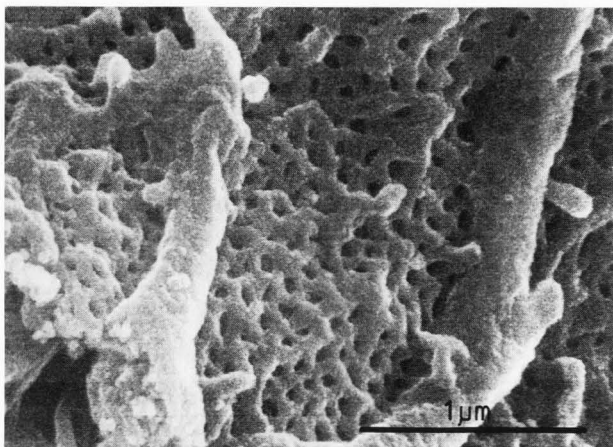
Fig. 9b SE image at medium magnification. Good contrast equal to that seen in all other images after thick metal application. Small structural surface details are recognizable. (x 30,000).
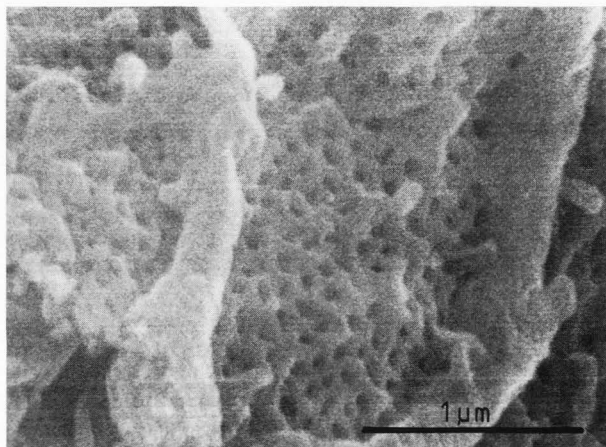
Fig. 9e BSE image at medium magnification. The noise in the signal is increased by comparison with that in the BSE image of a 10 nm gold decorated specimen (see figure 5e). (x 30,000).
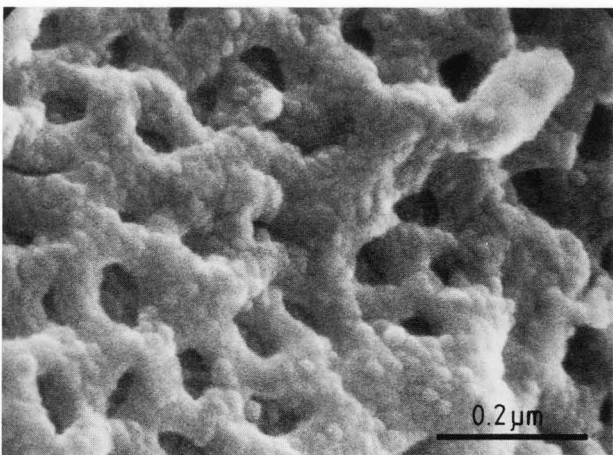
Fig. 9c SE image at high magnification. Outstanding signal with low noise enriched in SE-I. Excellent topographic contrasts. Closely packed particles appear in the image. (x 100,000).
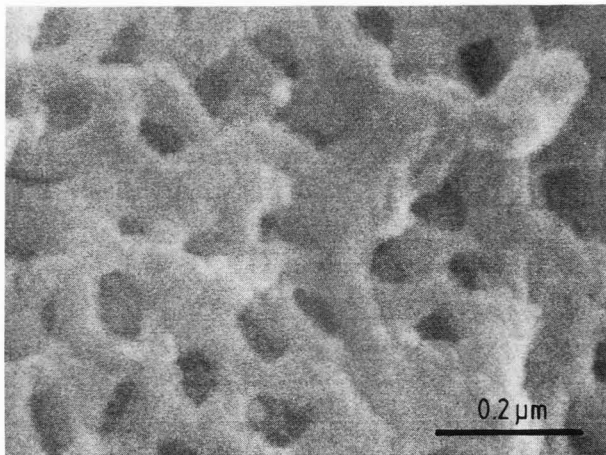
Fig. 9g BSE image at high magnification. Excellent BSE resolution of some 15 - 20 nm large surface particles. However, only few of the SE contrasts (figure 9c) are matched. (x 100,000).

recognizable SE-I edge brightness added high resolution contrasts to the image of the platinum decorated surface. Obviously, the improved continuity of the platinum film caused a reduction in background signal and an increase of SE-I/SE-II ratio (Peters, 1982b). This effect of film continuity became more evident when other metals of finer grain structure were used.

Specimens Coated with Continuous Metal Films.

Metals which coat surfaces form continuous, very compact films at an average mass thickness of of 1 - 2 nm. They consist of very small metal aggregates which are not resolved at high magnification (Peters, 1986). These films improve the contrasts at high magnifications.

5 nm Thick Tantalum Coating. The low magnification SE image (Fig. 9a) was similar to the backscattered image of thicker gold films; both indicated a lack of contrast of 100 - 200 nm large features. However, at medium magnification (Fig. 9b) very good images with recognizable fine structures were produced. At high magnification

Fig. 10a   Specimen coated with a 1 nm thin continuous film of chromium. SE image. Little particle contrast and edge contouring indicative of a small signal exit area. (x ∿ 1,000).

Fig. 9f BSE image of the same area as shown in figure 9e. The signal, produced only from the specimen grid, accounts for ∿20% of the total SE-III signal generated by the converter.
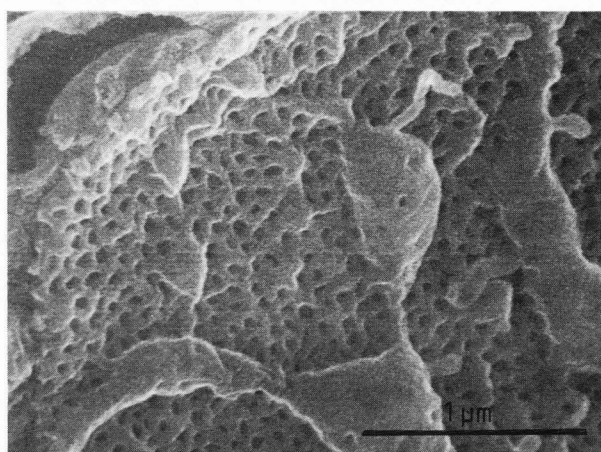

Fig. 10b   SE image at medium magnification. Similar contrast as in images of specimens with thick metal applications (figure 5b). Topographic SE-I contrasts are barely visible. (x 30,000).

(Fig. 9c) an excellent image of the metal surface was routinely obtained. Surprisingly, the S/N ratio was drastically increased when compared with the images of gold decoration of the same thickness (see Fig. 6c). The metal film was smooth and revealed a distinct topographic substructure, seen as 15 - 20 nm large particles and imaged with distinct sharp outlines and close apposition. Excellent topographic contrasts were seen which included relief contrast as well as thin edge brightness. The continuity and compactness of the film prevented generation of micro-roughness background signal and increased the SE-I/SE-II ratio.

The BSE signal from this tantalum coating complemented the SE contrast only to a certain extent. At low magnification (Fig. 9d) a very similar image was obtained as after 10 nm gold application (see Fig. 5d). However, at higher magnifications the BSE signal was weaker and expressed a lower S/N level. Even at medium

Fig. 10c   SE image at high magnification. Imaging of small surface features outlined by a thin contour in SE-I contrast. The details are not revealed by other metal applications. (x 100,000).

magnification it became obvious that the BSE contrasts did not match all SE contrasts imaged at the same magnification (see Fig. 9b) although the BSE signal, compared to the SE signal, was approxi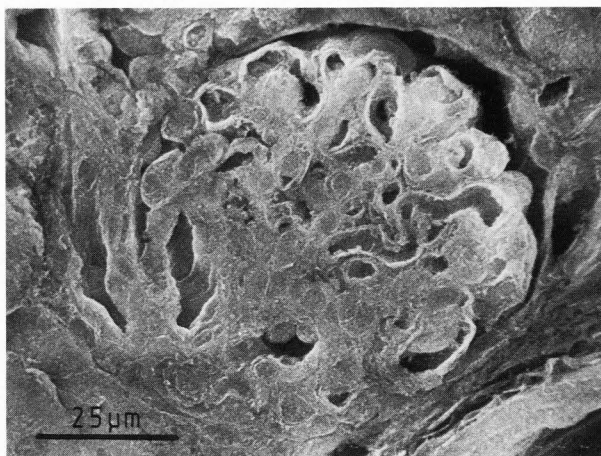mately 60% stronger with a high signal contribution from the specimen grid used for the BSE imaging (Fig. 9f). Also, the BSE produced, at high magnification, an excellent resolution, since the 15 - 20 nm surface structures of the metal film were resolved in some areas. However, comparison of BSE and SE contrasts in the high magnification image revealed that not all SE contrasts were matched by BSE contrasts. Most of the material contrast (cell surface versus fenestrae) originated from SE-II but nearly all topographic contrasts contained a strong SE-I contribution. The improved resolution intuitively justified the impression that the cell surface was blanketed by an extensive thick layer of metal.

1 nm Thin Chromium Coating. Very thin continuous chromium coatings produced very different contrast patterns on these specimens. At low magnification (Fig. 10a) only very little contrast was generated by scattered PE. The image was quite similar to the BSE image produced by 8 keV PE (see Fig. 5i) and was characterized by very crisp contours of small details but also by a very flat contrast of larger features like the tubule walls.

At medium magnification (Fig. 10b) the particle contrasts of larger features like the fenestrated cell body or its cytoplasmic ridges showed only very little topographic contrasts similar to the image after a 10 nm thick gold decoration (Fig. 5b). However, already at this magnification a very thin edge contouring became reco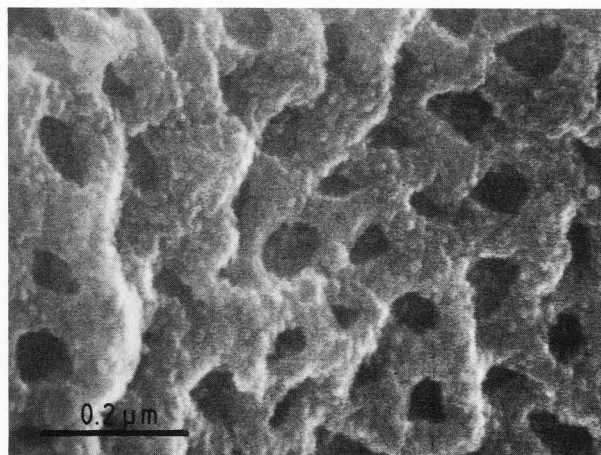gnizable but no other details were visible on the cell surface. At high magnification (Fig. 10c) contrast of small structures, not imaged by any other metal film, became a dominant image element. Small, 6 - 8 nm wide rods stand 15 - 20 nm tall in ∿10 nm distance on the luminal surface of the cell and are well contoured by 1 nm wide bright lines.

The surface particle's contour was as bright as the outlining of the fenestrae and other elevated larger features. The BSE signal from this specimen was smaller than the SE signal and showed contrasts very similar to the uncoated specimen (see. Fig. 4). The majority of the contrasts imaged at medium and high magnification (Figs. 10b and c) were generated by the type I signal. If compared to the uncoated specimen (see Fig. 4c) the 1 nm thick chromium film did indeed enhance the contrast of the membrane surface as well as the surface fine structures without distorting the topographic aspect of the specimen. The excitation volume of the SE was reduced to the metal film thickness and the resolution was improved as predicted (Everhart and Chung, 1972).

Conclusions

This paper describes the preparative conditions which are necessary to generate high resolution SE-I contrasts for the imaging of macromolecular fine structures on cell surfaces in complex biological specimens. The imaging methodology used here includes: i) tissue preparation, ii) contrast enhancement and iii) high resolution microscopy. In this paper, the second part was experimentally analyzed and the conditions for achieving high resolution on biological specimens were defined.

Working at Higher Magnifications.

The use of a scanning electron microscope at high magnification differs very much from conventional scanning microscopy. First, high brightness guns, like field emitters, provide a small beam diameter over a wide range of beam currents and allow work within a wide range of magnifications <300,000 x without readjusting apertures, working distances or beam currents. However, in standard microscopes signal collection must be corrected to establish the SE-I imaging mode in which all type III signals are eliminated (Peters, 1982a and 1984b). Then, high accelerating voltage is used to establish the smallest beam diameter and highest gun brightness and to reduce the background signal contrast. Low voltage microscopy (Pawley, 1984), although exciting, has not yet been able to demonstrate any high resolution contrast of a type I signal either on small isolated particles, i.e., bright edge contrast on small gold particles, or on bulk specimen, i.e., solid gold (Peters, 1984b) or uncoated organic material (as demonstrated in figure 4c).

It is most helpful to use standard specimens for evaluation of techniques suitable for high magnification imaging. Slices of rat or mouse kidney are an easily accessible biological specimen and have already proved very suitable to demonstrate new imaging approaches, i.e., OTO-coating (Komoda and Saito, 1972; Murakami, 1978) or quick-freezing approaches (Bearer et al., 1985). Comparison of different TEM and SEM high magnification imaging techniques should be done with micrographs of identical but high magnifications since metal decoration effects and type I contrasts occur mostly at specimen features of very small size.

At lower magnifications, the contrast will be reduced in proportion with the square of the pixel radius and its relative image size will increase (Fig. 3d). However, since the image is produced with an unchanged number of scans, the probe might even miss at low magnifications certain features which might completely disappear from the image. At higher magnification when several pixels image the feature, the S/N ratio increases to the point that even details in contrast distribution within the edge brightness become recognizable, for example, the very high intensity bright outline within 1 nm from the edge (Joy, 1984). Such features may be imaged only above 200,000 x (Fig. 3e). Too high a magnification will not reveal any further details and may lead into problems of quite a different nature, like contamination deposition (Peters, 1984a) or beam damage (Peters, 1985b).

In conventional low magnification microscopy with type II signals the exit areas of the signals are very large so that already at ∿1,000 x magnification differences produced by changing accelerating voltage or coating thickness are recognizable. However, on biological specimens at very low magnifications (∿<100 x) these contrast

phenomena get less involved in the contrast generation and collection efficiency contrasts take over.

Generation of High Resolution Type I Signal Contrasts.

Biological specimens are conventionally fixed and dried for scanning microscopy. Such organic specimens are not different from other bulk but inorganic samples. They are characterized by the same properties: i) low specific density, i.e., $\sim$0.2 - 0.5 g/cm^3 (Becker and Sogard, 1979; Pawley, 1984); and ii) low average atomic number composition, which is $\sim$7 (Joy, 1984; Pawley, 1984). In contrast to many inorganic samples, dried biological specimens have only low electrical conductivity. An elegant way to improve the conductivity but not to bury surface fine structures was found in their impregnation with osmium black (Hanker et al., 1964) which should be applied, however, in a controlled way so as carefully to avoid the conventional osmium black coating.

Such specimens made possible high magnification imaging even without metal application and revealed type I signal contrasts (Fig. 4c) which were similar to those imaged on bulk inorganic materials, i.e., lanthanum hexaboride (Broers, 1969) or carbon (Koike et al., 1973). However, only the strongest of the topographic contrast, the edge brightness, was imaged. Relief contrast and contrasts produced at small surface features, i.e., particle contrast, were too weak to be recognized. Resolution on bulk specimen is also limited by the exit area from which the SE-I signal electrons are emitted and which has a diameter equal to twice the range plus the beam diameter. SE range in low atomic number specimens is several nm so that only a low resolution can be expected. Thus, metal application was needed to increase contrast and resolution. With thin metal films, $\sim$1 - 2 nm in thickness, all topographic contrasts can be demonstrated (Peters, 1984b) and the contrast produced on organic specimens can become equal to that imaged by a type I signal on bulk inorganic specimens, like gold.

On a biological surface, the metal film produces mainly a strong contrast at edges so that features larger than 1 - 2 nm are imaged outlined by a bright contour. So many details are revealed on cell surfaces that stereoscopic viewing is necessary to analyse the two-dimensional projection images in which the three-dimensional topographic relation of contrasts and structural features may be obscured (Fig. 11). Small elongated features, $\sim$6 - 8 nm in width and $\sim$15 - 20 nm high, are standing on the membrane surface spaced by $\sim$10 - 15 nm. These rod-like structures may represent the ectodomains of membrane glycoproteins. They are only found on the luminal surface and are absent at the circumferential walls of the fenestrae. Relief contrast is very weak and it is recognizable only at the transition from the luminal surface to the fenestral openings. The cell surface itself is imaged with a material contrast component, against the openings of the fenestrae - but a type II particle contrast component may also contribute to the contrast. Smaller features (2 - 5 nm) attached to the

membrane are imaged as fuzzy bright disks since the thin metal film may be already too "thick" to contour them and since the S/N ratio of the type I signal becomes too low.

The application of metal introduces additional problems limiting the topographic resolution, because it is the metal film and not the specimen's surface which is imaged (Revel, 1978). Certain properties of the metal film cause effects which reduce the resolution (Peters, 1985b). The three most important are: i) blanketing of small features by excessive film thickness, ii) decoration of surface features instead of coating them so that final metal accumulations enhance only certain surface sites, and iii) deterioration of high magnification contrasts by an increased background signal caused by film discontinuities.

The origin and the reduction of the background signals were already discussed in the previous section. The effects of the conventional application of metal films on contrast enhancement of fine structures can be identified now because the "true" surface fine structure can be revealed with the type I signal contrasts.

Coating with Excessive Metal.
Thick metal films obscure small surface structures. The film thickness should not exceed the smallest dimension to be visualized (Moor, 1959). For high resolution microscopy a $\sim$1 nm film thickness is appropriate. Conventionally, $\sim$5 - 10 nm thick metal layers are used to generate, at higher magnifications, a sufficient signal for conventional (signal type II) scanning microscopy and $\sim$3 - 5 nm of platinum-carbon are used to produce quick-frozen, deep-etched replicas for conventional transmission microscopy. If such high amounts of metal are distributed evenly in a coating fashion, the surface becomes "blanketed by metal". A 5 nm thick film of tantalum deposited by multidirectionally tumbling on the surface fine structures (Fig. 12) increased their diameter by 10 nm to 16 - 18 nm. Actually, since the fine structures were 15 - 20 nm high and spaced at a distance of $\sim$10 nm, the base of the rod-like features was shadowed from the metal source by surrounding features and received less metal. However, the particle's top was coated by the full amount so that the tips enlarged and touched each other, forming a continuous surface. Particles on the cell surface (and fibers of the basement membrane) standing out were coated on all exposed sides. If the particle tops were closer to each other than 10 nm, the metal film would grow to a continuous smooth layer hiding the particles beneath. In fact, over several areas such smooth surface is recognizable. The excessive metal coating reduced surface information (see Fig. 11) to a mere center-to-center spacing of selective particles sufficiently elevated above the outer-most surface plane. Particle sizes may be calculated from the coating thickness. Viewing figures 11 and 12 side-by-side and with the same magnification reveals the advantages of the new imaging approach. Whereas figure 11 reveals cell surface structures (since the metal coating is thinner than the fine structures are wide), figure 12 indicates only metal structures (since the metal coating is equal to or thicker than the
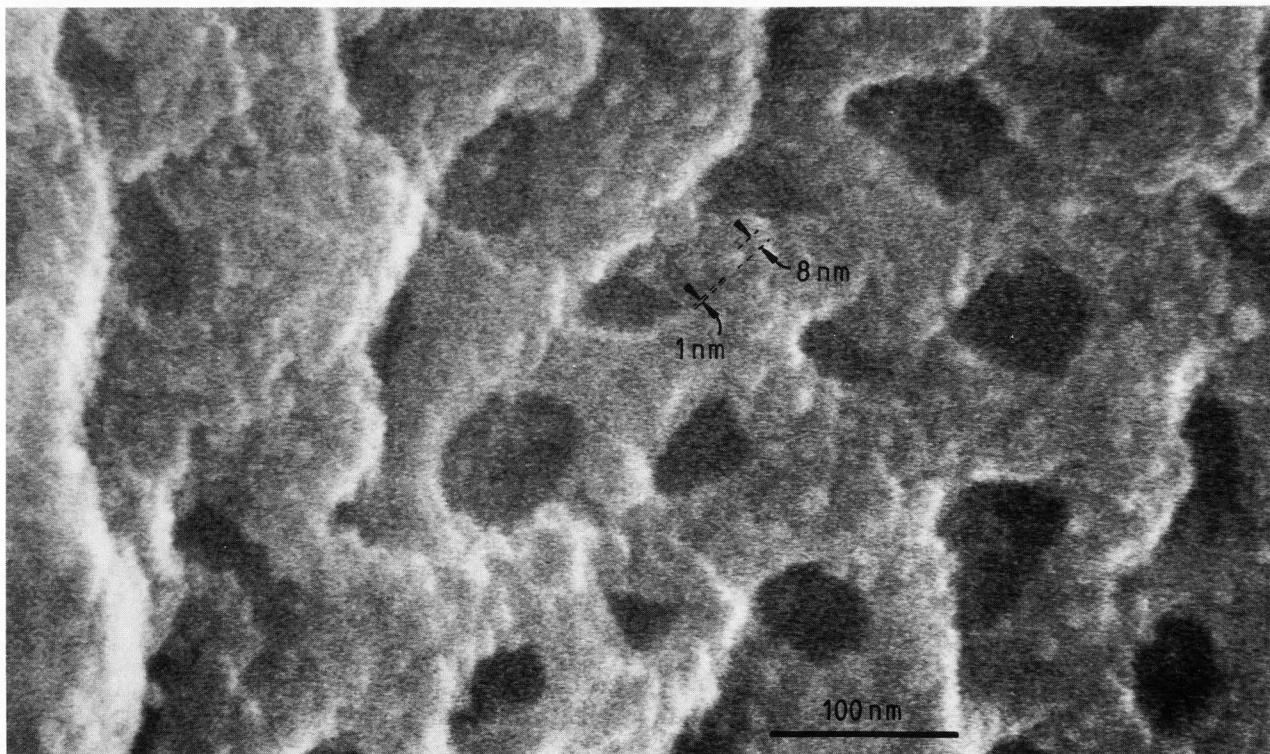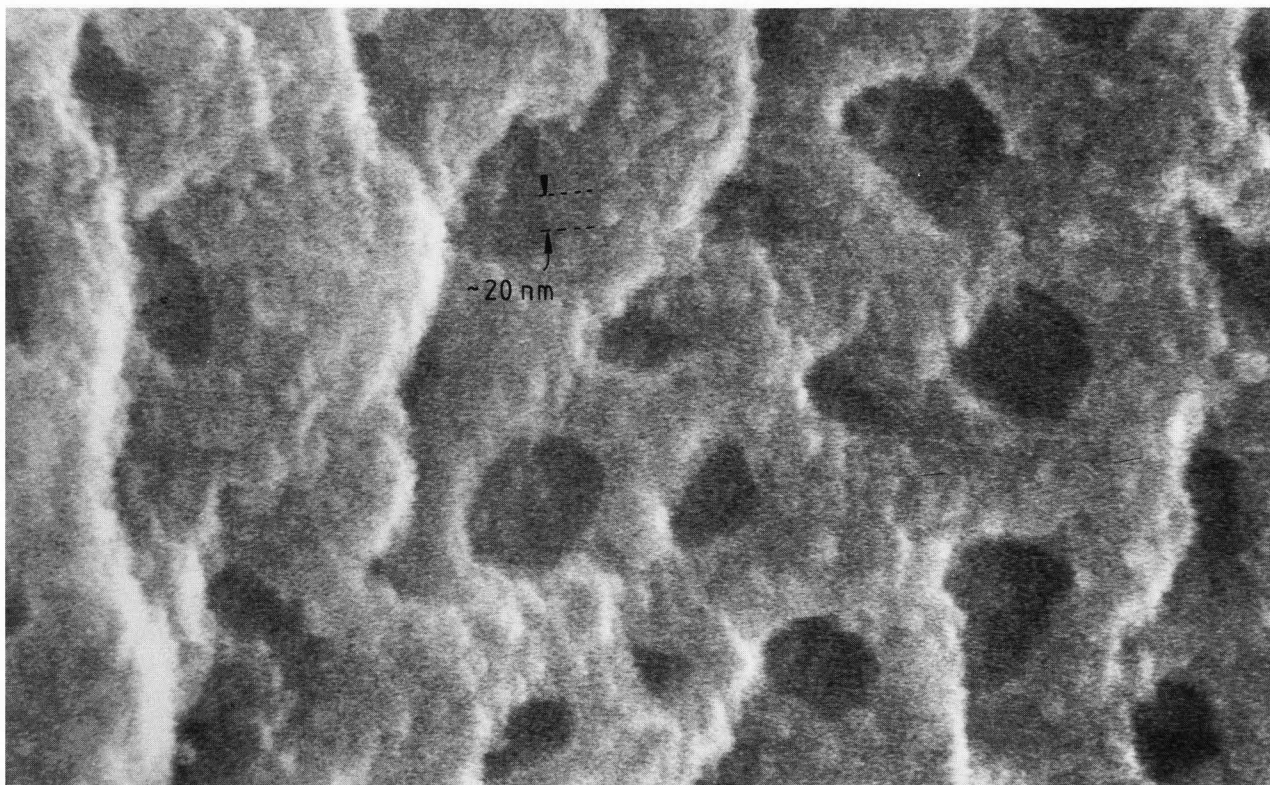
Fig. 11 High quality high magnification image of a cell surface coated with a 1 nm thin continuous Cr film. Please hold stereo prisms (System Nesh, see Materials and Methods) with right hand. Compare with figure 12. Size, shape, orientation and spacing of individual (or clustered) ectodomains of membrane glycoproteins are imaged in SE-I contrast on the luminal surface only. (x 250,000).

Stereo-micrographs are mounted vertically for viewing with stereo prisms only.

17 nm

100 nm
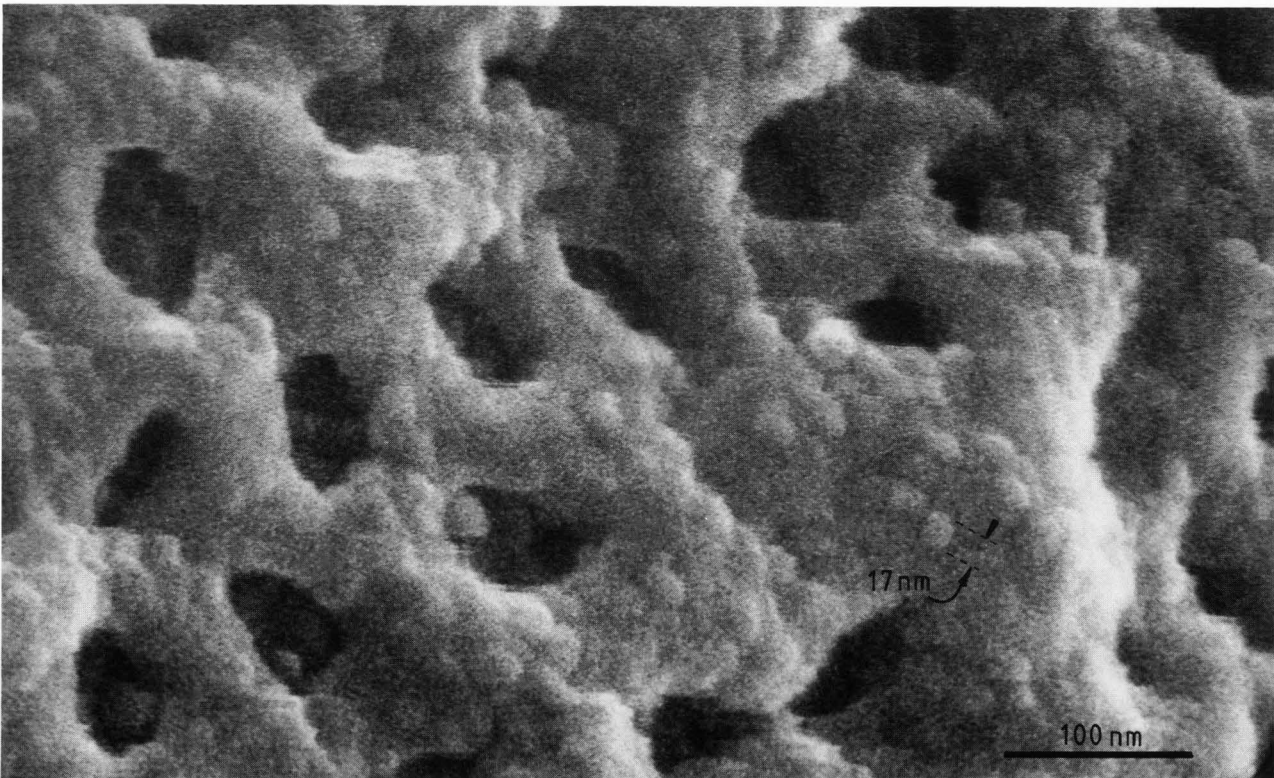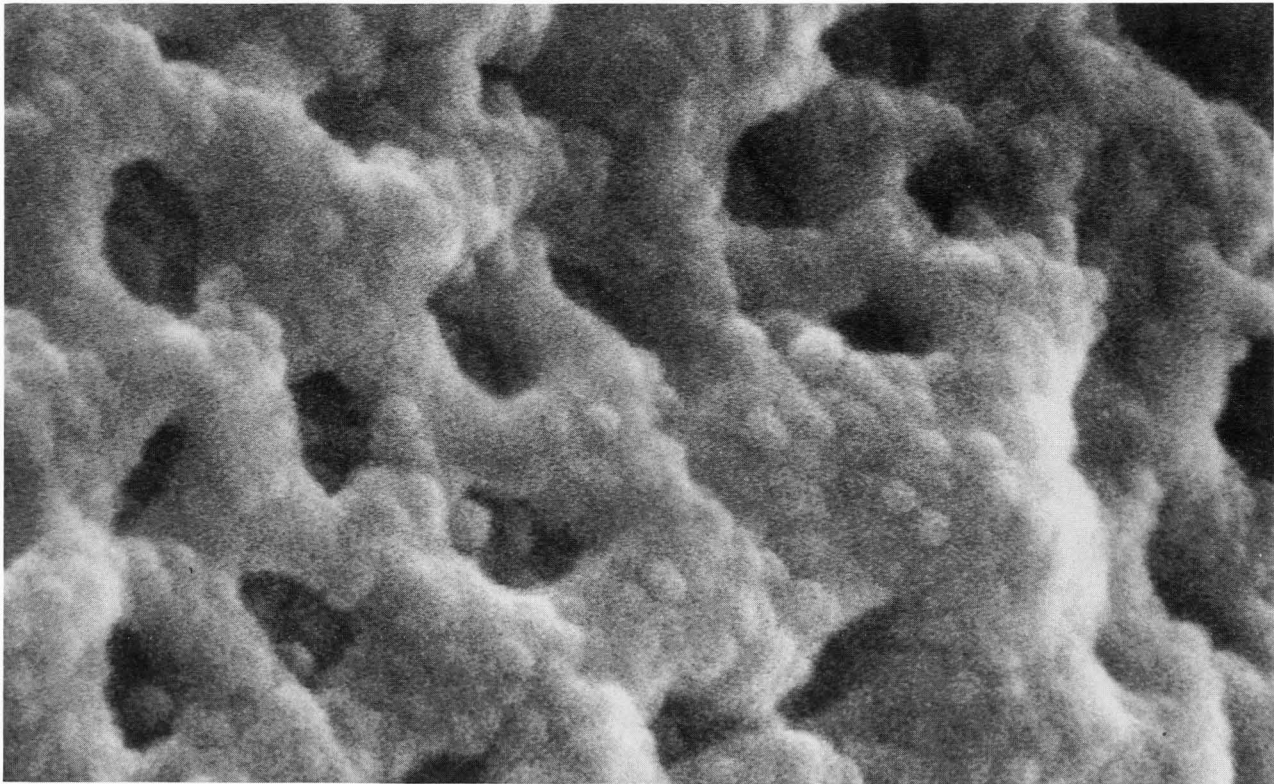
Fig. 12 High magnification SE image of similar cell surface blanketed under a 5 nm thick continuous coating with Ta. Compare with figure 11. High quality SE image enriched in type I contrasts. However, the heavy metal blanket obscures most of the topographic features except for center-to-center spacings and particle size (enlarged by 2 x metal coat thickness). (x 250,000).
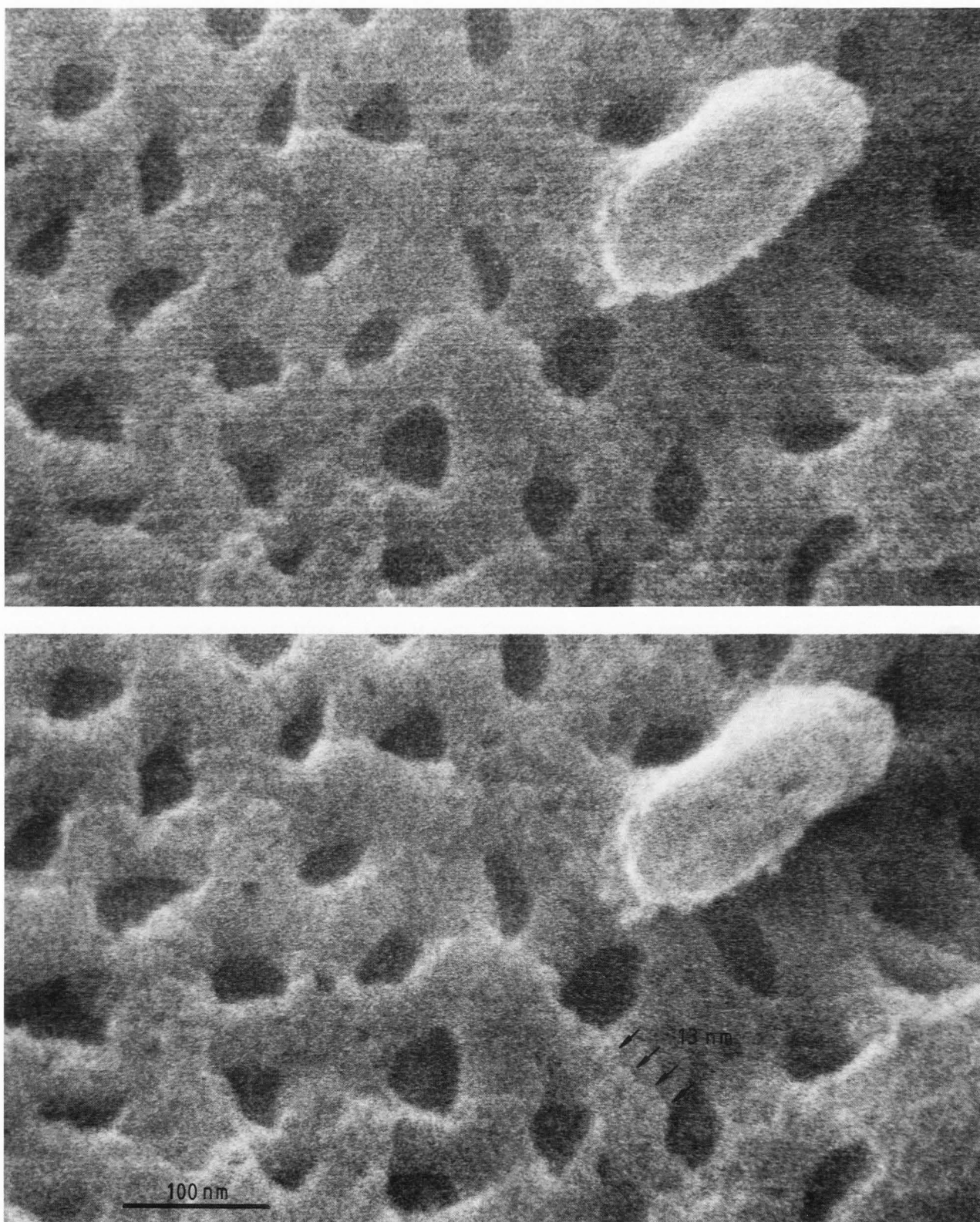
Fig. 13 Low quality SE image of cell surface decorated with a 5 nm thick discontinuous gold film. The loosely packed metal aggregates produce a high background signal (SE-II micro-roughness contrast) which deteriorates the SE-I signal from the metal aggregates accumulated on top of the surface structures. Only information on center-to center particle spacing is available. Compare with figure 12.   (x 250,000).

276

Fig. 14 High magnification SE image of cell surface buried under 10 nm continuous gold decoration: all information on surface structure is lost. The type II signal at improved S/N ratio (compared to figure 13) images the cell body in particle contrast. Small spots high in contrast represent metal substructures but not structural details of the biological surface. (x 250,000).

dimensions of the features to be imaged). This obvious difference in surface information is lost or becomes uncertain if decoration occurs.

Decoration with Gold and Platinum. Thick metal accumulations distort the topography as well as the redistribution of the metal during its deposition, thereby generating decoration of surface features.

Conventionally gold and platinum are used also for high magnification imaging. However, in such cases the phenomenon of decoration is often not recognized. Metal atoms of high surface mobility deposited under conventional conditions diffuse on the surface and accumulate at sites different from their point of arrival. The sites of accumulation (nucleation sites) are determined by properties of the metal and of the surface (Basset, 1958; Bachmann et al., 1960; Peters, 1979). The accumulation sites on biological surfaces are, as a rule, elevated small particles (Peters, 1979 and 1982b). The 5 nm (average) mass thickness of gold deposited under the same conditions as the tantalum discussed before, produced on the cell surface a metal distribution pattern (Fig. 13) very different from the tantalum coating. The gold accumulated on top of the surface fine structures into large aggregates and formed a discontinuous layer. It overgrew the lateral dimensions of the particles and bridged the gaps between their tops. If a neighboring particle was missing a hole remained in the growth plane of the metal aggregates.

These holes proved that the gold did not accumulate at the base or the vertical sides of the surface molecules. Most of the metal landing at the sides moved up to the top and accumulated into smaller aggregates. This resulted in an uneven distribution of the gold reflecting local nucleation site distributions. Knowing the real surface of the specimen (see Fig. 11) it is clear that the gold decoration displays only the center-to-center distance of the particles but does not reveal their individual shapes, widths, heights, spacings or orientations. Thus, decoration yields only part of the topographic information. This is its strength in the imaging of known surfaces (ionic salt lattices) but is its downfall on unknown surfaces of biological specimens, membranes included.

Decoration with thick continuous gold layers 10 nm in thickness (Fig. 14) overgrew the individual nucleation sites, seen in the 5 nm thick deposition, and filled most of the remaining holes. The surface appeared smooth with all topographic fine structures buried under metal, leaving no reminder of their existence at the surface.

Frequently, in thin platinum films used for decoration, metal is deposited in such high amounts that continuous films are produced. Such films decorate the surface features as do the gold films. Accordingly, platinum films reveal little from the true three-dimensional surface information, i.e., no vertical dimensions smaller than the diffusion range of the metal (Peters, 1986) can be imaged. Since platinum or platinum-carbon accumulates (above 100 K) into somewhat smaller clusters than gold, a decorated surface may reveal smaller structures. The images may give the impression of improved resolution, but in fact they indicate only a finer decoration still affected by all the limitations mentioned above.

A 1 - 2 nm thick platinum film is discontinuous (Fig. 15). Individual platinum clusters are recognizable on the cell surface in a lateral distribution pattern with spacings equal to the center-to-center distance of the molecules. Again, no metal accumulated at the vertical sides of the surface features to give an image of their shapes and sizes. However, fibers, spanned beneath the fenestrae in the basement membrane, were recognized by the metal since freedom of diffusion is restricted to the length of the fibers and less metal can accumulate by diffusion.

Background Signal. Films of loosely packed metal aggregates, like gold or platinum films (see Figs. 13 - 15), produce a higher signal than compact continuous films of small aggregates, like tantalum films (see Fig. 12). The scattered PE generate in the local vicinity of the probe's site a type II signal which carries a contrast that depends on the local scattering conditions. This contrast contribution, referred to as micro-roughness contrast (of the type I signal), degrades the contrasts of the type I signal in a similar way as the type III background signal does (Peters, 1984a). The micro-roughness contribution is fully suppressed when continuous films of small metal aggregates are used. This is a further important reason to avoid the use of gold or platinum in high magnification scanning work.

However, at low magnification when a pixel represents a surface area equal to the exit area for micro-roughness contrast, the increased signal contributes usefully to the image and increases the contrast of small features 100 - 200 nm in size (see Figs. 6a, 8a and compare with Fig. 9a).

Application of High Resolution Imaging.

High resolution SEM can now overcome the limitations imposed by platinum to TEM and combine advantages of conventional scanning electron microscopy with a resolution higher than is obtained on TEM replicas of quick-frozen, deep-etched or dried specimens. A platinum-carbon replica of a similar specimen as imaged here in SEM (after critical-point drying) could not reveal any molecular membrane structures or any equivalent features on glomerular endothelial cell surfaces even though the specimen was prepared by quick-freezing and deep-etching (Bearer et al, 1985). The cell surface was replicated as a completely smooth plane lacking any details. A continuous platinum-carbon film can decorate and blanket the membrane surface as demonstrated in detail in the present study. (In contrast, on platinum decorated surfaces SEM was able to image at least the decoration sites with a micro-roughness contrast (Fig. 15), which is not generated in TEM).

The progress made with the new SEM high resolution imaging method using thin continuous coatings and a SE-I signal contrast becomes obvious when the TEM and SEM images are compared side-by side. Moreover, SEM can image large or extensively convoluted surfaces not accessible to replication, i.e., cell surfaces in tissues. The high tilting capability (up to ±90°), the greater depth of focus (due to a smaller illumination
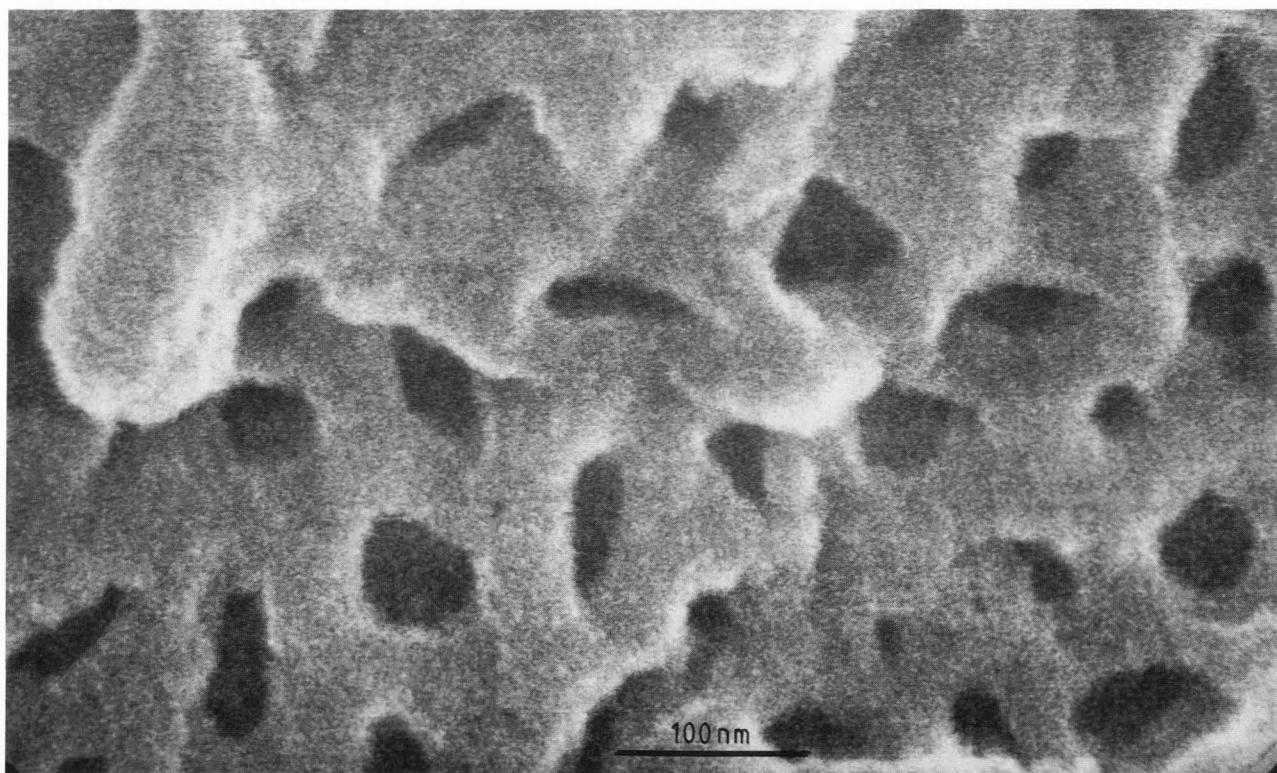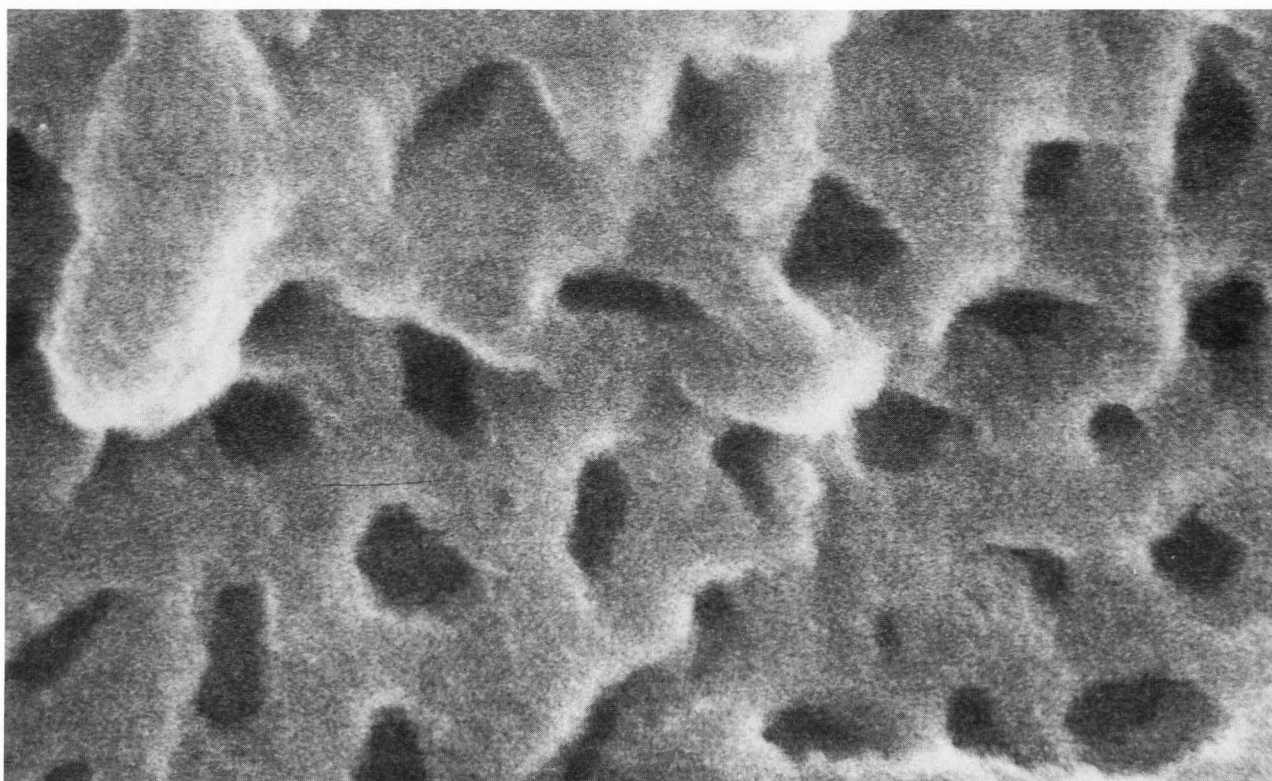
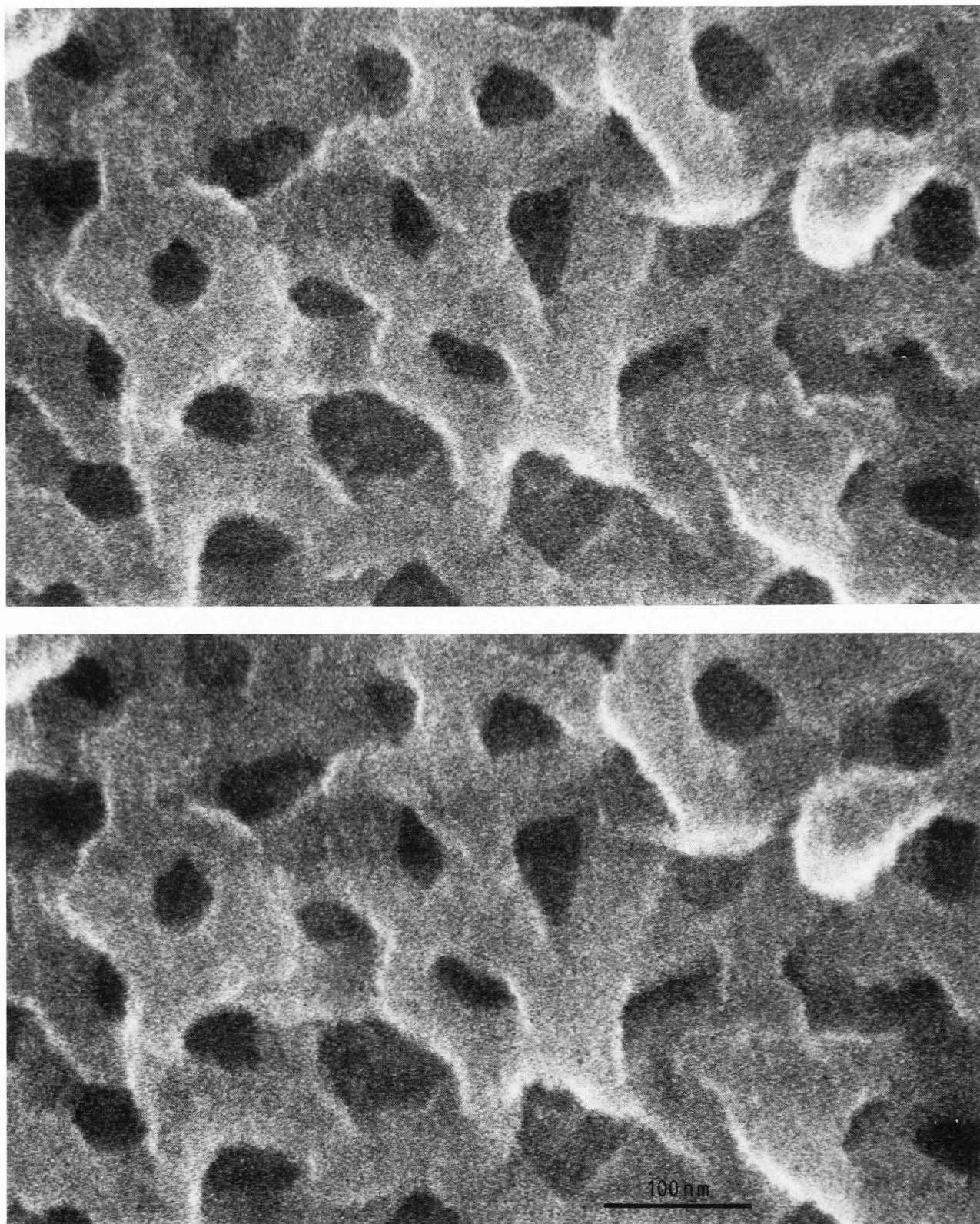Fig. 15   High magnification SE image of cell surface decorated with 1 - 2 nm thick discontinuous film of Pt. High noise level, produced by micro-roughness contrast, obscures the contrast generated by the decoration.   Platinum is no choice for high magnification imaging since it decorates (as gold does) and produces a background noise as high as generated by a 10 nm thick gold application. (x 250,000).

aperture) and the possibility of refocusing the image during its scan (dynamic focussing) make possible a clearer presentation of three-dimensional molecular structures of biological specimens. Stereoscopic imaging is as valuable at high magnifications as it has already proven to be in TEM and for low magnification imaging in conventional SEM.

The SEM preparation techniques include exposure of biological surfaces, controlled osmium impregnation, drying and metal coating at ambient temperatures, and are much simpler (and easier to automate) than the production of quick-frozen, deep-etched replicas of fractured frozen materials. Scanning microscopy gives easy access to selected specimen areas. On the kidney slices used in this study, imaging of endothelial cell surfaces in glomerular capillaries was facilitated by the fact that a dozen glomeruli were accessible on each kidney slice and on each glomerulus several exposed capillaries could be preselected in minutes.

Since SEM images the metal film on the specimen surface without any further processing, a free choice of any kind of metal is possible, i.e., high or low atomic numbers suitable to coat rather than to decorate. Coating provides direct access to unknown fine structures not to be revealed after decorating.

The high resolution imaging mode used in this study for all micrographs improved the image contrast also at medium magnifications and thereby made possible the recognition of more specimen details than detectable by conventional SEM. With these new procedures it was possible to describe new biological structures in a variety of tissues, i.e., the periciliary ridge complex in retinal rod cells (Peters et al., 1983), endothelial pockets in capillaries (Peters and Milici, 1985), as well as subcellular structures, i.e., striped vesicles (Peters et al., 1985) and pores in diaphragms of capillary endothelium (Peters and Milici, 1983).

The application of high resolution SEM in life sciences and clinical diagnosis will depend on the establishment of a solid data base of macromolecular structures of cells and tissues and their alteration by pathological conditions. Such new data will complement information on cytoplasmic fine structures of cells or cell-to-cell interactions obtained by the now well established TEM sectioning approach. However, high magnification SE-I SEM has the potential advantage of easy access to specific and important three-dimensional structural elements of cells and tissues not seen in TEM sections.

Acknowledgements

References

Bachmann L, Orr WH, Rhodin TN, Siegel BM (1960). Determination of surface structure using ultra-high vacuum replication. J. Appl. Phys. 31: 1458-1462.

Basset GA (1958). A new technique for decoration of cleavage and slip steps on ionic crystal surfaces. Phil. Mag. Series VIII, Vol. 3: 1042-1045.

Baumann W, Reimer L (1981). Comparison of the noise of different electron detection systems using a scintillator-photomultiplier combination. Scanning 4: 141-151.

Bearer EL, Orci L, Sors P (1985). Endothelial fenestral diaphragms: a quick-freeze, deep-etch study. J. Cell Biol. 100: 418-428.

Becker RP, Sogard M (1979). Visualization of subsurface structures in cells and tissues by backscattered electron image. Scanning Electron Microsc. 1979;II: 835-870.

Boyde A, Cowham NJ (1980). An alternative method for obtaining converted backscattered electron images and other uses for specimen biasing in biological SEM. Scanning Electron Microsc. 1980;I: 227-232.

Broers AN (1969). Some experimental and estimated characteristics of the lanthanum hexaboride rod cathode electron gun. J. Sci. Instrum. (J. Phys. E) 2: 273-276.

Broers AN (1970). Factors affecting resolution in the SEM. Scanning Electron Microsc. 1970: 1-8.

Broers AN, Panessa BJ, Gennaro JF (1975). High resolution SEM of biological specimens. Scanning Electron Microsc. 1975: 233-242.

Crewe AV, Lin PSD (1976). The use of backscattered electrons for imaging purposes in a scanning electron microscope. Ultramicrosc. 1: 231-238.

Drescher H, Reimer L, Seidel H (1970). Rückstreukoeffizient und Sekundärelektronen-Ausbeute von 10-100 keV-Elektronen und Beziehungen zur Raster-Elektronenmikroskopie. Z. angew. Phys. 29: 331-336.

Echlin P (1972). The rationale and mode of application of thin films to non-conducting materials. Scanning Electron Microsc. 1972: 137-146.

Everhart TE, Thornley RFM (1960). Wide-band detector for micro-micro ampere low-energy electron currents. J. Sci. Instrum. 37: 246-248.

Everhart TE, Chung MS (1972). Idealized spatial emission distribution of secondary electrons. J. Appl. Phys. 43: 3307-3311.

Everhart TE, Wells OC, Oatley CW (1959). Factors affecting contrast and resolution in the scanning electron microscope. J. Electr. a. Control 7: 97-111.

George EP, Robinson VNE (1976) The dependence of

SEM contrast upon electron penetration. Scanning Electron Microsc. 1976;I: 17-26, 738.

George EP, Robinson VNE (1977a). Contribution to backscattered electrons discussion. Summary of our views. Scanning Electron Microsc. 1977;I: 773-774.

George EP, Robinson VNE (1977b). The influence of electron scattering on the detection of fine topographic detail in the scanning electron microscope (SEM). Scanning Electron Microsc. 1977;I: 63-70, 31.

Hanker JS, Seaman AR, Weiss LP, Ueno H, Bergman RA, Seligman AM (1964). Osmiophilic reagents: new cytochemical principle for light and electron microscopy. Science 146: 1039-1043.

Hasselbach F, Rieke U (1976). Emission microscopical investigation of the edge brightening effect in scanning electron microscopy. 6th European Congress on Electron Microscopy. Tal Pub. Co., Jerusalem; Vol. 1: 296-298.

Horrisberger M, Rosset J (1977). Colloidal gold, a useful marker for transmission and scanning electron microscopy. J. Histochem. and Cytochem. 25: 295-305.

Jacopic E, Brunegger A, Essl R, Windisch G (1978). A sputter source for electron microscopic preparation. In: Sturgess JM (Ed.), Electron Microscopy 1978. Microscopical Society of Canada, Toronto; Vol. I Physics: 150-151.

Joy DC (1984). Beam interactions, contrast and resolution in the SEM. J. Microsc. 136: 241-258.

Kanter H (1957). Zur Rückstreung von Elektronen im Energiebereich von 10 bis 100 keV. Ann. Physik. 20: 144-166.

Kanter H (1961a). Energy dissipation and secondary electron emission in solids. Phys. Rev. 121: 677-681.

Kanter H (1961b). Contribution of backscattered electrons to secondary electron formation. Phys. Rev. 121: 681-684.

Kawamoto H, Yamazaki S, Ishikawa A, Buchanan R (1984). Effects of secondary electron detector position on scanning electron microscope image. Scanning Electron Microsc. 1984; I: 15-22.

Kelley RO, Decker RAF, Bluemink JG (1973). Ligand-mediated osmium binding: its application in coating biological specimens for scanning electron microscopy. J. Ultrastruct. Res. 45: 254-258.

Koike H, Ueno K, Suzuki M (1971). Scanning device combined with conventional electron microscope. Twenty-ninth Annual Meeting Electron Microscopy Society America. Claitor's Publ. Div., Baton Rouge, LA: 28-29.

Koike H, Namae T, Watabe T, Milkajiri A (1973). An approach to microanalysis with the electron microscope. JEOL News 10e;4: 2-8.

Komoda T, Saito S (1972). Experimental resolution limit in the secondary electron mode for a field emission source scanning electron microscope. Scanning Electron Microsc. 1972: 129-136.

Lin PDS, Becker RP (1975). Detection of backscattered electrons with high resolution. Scanning Electron Microsc. 1975: 61-70.

Moll SH, Healey F, Sullivan B, Johnson W (1978). A high efficiency, nondirectional backscattered electron detector. Scanning Electron Microsc. 1978;I: 303-310.

Moll SH, Healey F, Sullivan B, Johnson W (1979). Further developments of the converted backscattered electron detector. Scanning Electron Microsc. 1979;II: 149-154.

Moncrieff DA, Barker RP (1978). Secondary electron emission in the scanning electron microscope. Scanning 1: 195-197.

Moor H (1959). Platin-Kohle-Abdruck-Technik angewandt auf den Feinbau der Milchröhren. J. Ultrastruc. Res. 2: 393-422.

Murakami T (1978). Tannin-osmium conductive staining of biological specimens for non-coated scanning electron microscopy. Scanning 1: 127-129.

Murata K (1973). Monte Carlo calculations on electron scattering and secondary electron production in the SEM. Scanning Electron Microsc. 1973: 267-276.

Niedrig H (1978). Physical background of electron backscattering. Scanning 1: 17-34.

Ong PS (1970). Contrast and resolution in scanning electron microscopy using backscattered electrons. Twenty-eighth Annual Meeting Electron Microscopy Society America. Claitor's Publ. Div., Baton Rouge, LA: 392-393.

Pawley J (1984). Low voltage scanning electron microscopy. J. Microsc. 136: 45-68.

Peters K-R (1979). Scanning electron microscopy at macromolecular resolution in low energy mode on biological specimens coated with ultra thin metal films. Scanning Electron Mircosc. 1979;II: 133-148.

Peters K-R (1980a). Improved handling of structural fragile cell-biological specimens during electron microscopic preparation by the exchange method. J. Microsc. 118: 429-441.

Peters K-R (1980b). Penning sputtering of ultra thin films for high resolution electron microscopy. Scanning Electron Microsc. 1980;I: 143-154.

Peters K-R (1982a). Validation of George and Robinson SE-I signal theorem. Implication for ultrahigh resolution SEM on bulk untilted specimens. In: Bailey GW (Ed.), Fortieth Annual Meeting Electron Microscopy Society America. Claitor's Publ. Div., Baton Rouge, LA: 368-369.

Peters K-R (1982b). Conditions required for high quality high magnification images in secondary electron-I scanning electron microscopy. Scanning Electron Microsc. 1982: 1359-1372.

Peters K-R (1984a). Generation, collection and properties of an SE-I enriched signal suitable for high resolution SEM on bulk specimens. In: Kayser DF, Niedrig H, Newbury DE, Shimizu R (Eds.), Electron Beam Interactions with Solids for Microscopy, Microanalysis and Microlithography. Scanning Electron Microscopy Inc., AMF O'Hare, IL 60666: 363-372.

Peters K-R (1984b). Scanning electron microscopy: Contrast at high magnification. In: Romig AD, Goldstein JI (Eds.), Microbeam Analysis - 1984. San Francisco Press Inc., San Francisco, CA. 77-80.*

Peters K-R (1985a). Noise reduction in high-magnification micrographs by soft focus printing and digital image processing. Scanning 7: 205-215.

Peters K-R (1985b). Rationales for the application of thin continuous metal films in high magnification electron microscopy. J. Microsc. (in press).

Peters K-R (1986). Metal deposition by high-energy sputtering for high magnification electron microscopy. In: Koehler JK (Ed.) Advanced Techniques in Biological Electron Microscopy III, Springer-Verlag Berlin-Heidelberg-New York (in press).

Peters K-R, Green SA (1983). Macromolecular structures of biological specimens are not obscured by controlled osmium impregnation. In: Bailey GW (Ed.), Forty-first Annual Meeting Electron Microscopy Society America. San Francisco Press Inc., San Francisco, CA. 606-607.

Peters K-R, Milici AJ (1983). High resolution scanning electron microscopy of the luminal surface of a fenestrated capillary endothelium. J. Cell Biol. 97:336a (abstract).

Peters K-R, Milici AJ (1985). Endothelial pockets are new transendothelial structures expressed by individual cells in renal fenestrated peritubular capilliaries. J. Cell Biol. 101: 110a (abstract).

Peters K-R, Palade GE, Schneider BG, Papermaster DS (1983). Fine structure of a periciliary ridge complex of frog retina rod cells revealed by ultrahigh resolution scanning electron microscopy. J. Cell Biol. 96: 265-276.

Peters K-R, Carley WW, Palade GE (1985). Endothelial plasmalemma vesicles have a characteristic striped bipolar surface structure. J. Cell Biol. 101; No. 6 (in press).

Reimer L (1978). Scanning electron microscopy - present state and trends. Scanning 1: 3-16.

Reimer L, Volbert B (1979). Detector system for backscattered electrons by conversion to secondary electrons. Scanning 2: 238-248.

Reimer L, Seidel H. Gilde H (1968). Einfluss der Elektronendiffusion auf die Bildentstehung im Raster-Elektronenmikroskop. Beitr. elektr. mikr. Direktabb. Oberfl. (BEDO Remey, Münster) 1: 53-65.

Revel JP (1978). Biological scanning electron microscopy for physicists and engineers. Scanning Electron Microsc. 1978;I: 829-834, 662.

Seiler H (1967). Einige aktuelle Probleme der Sekundärelektronenemission. Z. Angw. Phys. 22: 249-263.

Seiler H (1983). Secondary electron emission in the SEM. J. Appl. Phys. 54: R1-R18.

Siegel BM (1964). Modern Developments in Electron Microscopy. Academic Press, New York. p. 76.

Volbert B, Reimer L (1980). Advantages of two opposite Everhart-Thornley detectors in SEM. Scanning Electron Microsc. 1980;IV: 1-10.

Watabe T, Hoshino T, Harada Y (1976). Observation of individual ferritin particles in the secondary electron mode of scanning electron microscopy. A challenge to immunology using the JEM-100 C/ASID. JEOL News 14e,1: 11-14.

Wells OC (1971). Low-loss image for surface scanning electron microscope. App. Phys. Lett. 19: 232-235.

Wells OC (1974). Resolution of the topographic image in the SEM. Scanning Electron Microsc. 1974: 1-8, 320.

Wells, OC (1975) Measurements of low-loss electron emission from amorphous targets. Scanning Electron Microsc. 1975: 43-50, 132.

Wells, OC (1977). Backscattered electron image (BSI) in the scanning electron microscope (SEM). Scanning Electron Microsc. 1977;I: 747-771.

Wells OC (1979). Effects of collector take-off angles and energy filtering on the BSE image in the SEM. Scanning 2: 199-216.

Wells OC, Broers AN, Bremer CG (1973). Method for examining solid specimens with improved resolution in the scanning electron microscope (SEM). Appl. Phys. Lett. 23: 353-355.

Wells OC, Boyde, A, and Rezanowich A (1974). Scanning Electron Microscopy. McGraw-Hill Book Comp. New York.

* Please write publisher or author to obtain a technically fault-free reproduced reprint.